

**AN *IN VITRO* STUDY TO COMPARE COATINGS OF PEPTIDE AND  
COLLAGEN ON HYDROXYAPATITE COATED TITANIUM SURFACES**

**MOHSIN NAZIR**

**DISSERTATION SUBMITTED IN FULFILLMENT OF THE REQUIREMENTS FOR THE  
DEGREE OF  
MASTER OF DENTAL SCIENCES**

**FACULTY OF DENTISTRY  
DEPARTMENT OF RESTORATIVE DENTISTRY  
UNIVERSITY OF MALAYA  
KUALA LUMPUR  
2017**

**UNIVERSITY OF MALAYA**

**ORIGINAL LITERARY WORK DECLARATION**

Name of Candidate: MOHSIN NAZIR  
Registration/Matric No: DGC 140008  
Name of Degree: MASTER OF DENTAL SCIENCES.

Title of Project Paper/Research Report/Dissertation/Thesis:  
AN *IN VITRO* STUDY TO COMPARE COATINGS OF PEPTIDE AND COLLAGEN ON  
HYDROXYAPATITE COATED TITANIUM SURFACES.

Field of Study:

I do solemnly and sincerely declare that:

- (1) I am the sole author/writer of this Work;
- (2) This Work is original;
- (3) Any use of any work in which copyright exists was done by way of fair dealing and for permitted purposes and any excerpt or extract from, or reference to or reproduction of any copyright work has been disclosed expressly and sufficiently and the title of the Work and its authorship have been acknowledged in this Work;
- (4) I do not have any actual knowledge nor do I ought reasonably to know that the making of this work constitutes an infringement of any copyright work;
- (5) I hereby assign all and every rights in the copyright to this Work to the University of Malaya ("UM"), who henceforth shall be owner of the copyright in this Work and that any reproduction or use in any form or by any means whatsoever is prohibited without the written consent of UM having been first had and obtained;
- (6) I am fully aware that if in the course of making this Work I have infringed any copyright whether intentionally or otherwise, I may be subject to legal action or any other action as may be determined by UM.

Candidate's Signature

Date:

Subscribed and solemnly declared before,

Witness's Signature

Date:

Name:

Designation:

## ABSTRACT

**Introduction:** There is a paradigm shift in implantology in recent times. From implants being classically inert, and unable to interact with their environment, to them being biomimetic with the ability to affect their surroundings. Implants and more importantly, their surfaces, nowadays are designed to mimic nature. Therefore, the aim of this study was to compare the cell morphology, proliferation and differentiation of hydroxyapatite (HA) coated titanium surfaces biofunctionalized with RGD, and Collagen. **Objectives:** The first objective of the study was to modify the surface of the implant by gritting, sandblasting, and acid-etching the CPTi surfaces so that they are comparable to the commercially available implant surfaces. The second objective was to coat the modified surfaces with HA using a Simulated Body Fluid (SBF) solution so that a uniform layer of HA is formed on top of the samples. The third objective was to use physical adsorption for functionalizing RGD and Collagen on the HA/Tricalcium Phosphate coated CPTi surfaces. The final objective was to use the HA/Tricalcium Phosphate as the control to compare the *in vitro* response on the samples using human osteoblasts. **Methods:** There were three phases to this experiment, namely, the surface modification phase where gritting, sandblasting, and acid etching took place. The surface characterization phase, where the CPTi samples were coated with hydroxyapatite (HA) with simulated body fluid (SBF), RGD and collagen. The last phase was the *in vitro* phase where cell morphology, cell viability, cell proliferation and mineralization were assessed using human osteoblast cells (HOB) for the three different groups of surface coatings. **Results and Discussion:** The sandblasted samples showed an average roughness ( $S_a$ ) value of  $2.48 \pm 0.74\mu\text{m}$ . The acid-etched samples displayed a lesser roughness than their sandblasted counterparts, that is, an average  $S_a$  of  $2.35 \pm 0.18\mu\text{m}$ . Within the HA/Tricalcium phosphate coated samples, there was a general increase in  $S_a$  in all surfaces involved. The HA/Tricalcium phosphate coatings on the 14th day showed average

$S_a$  values of  $2.74 \pm 0.28\mu\text{m}$ . The average thickness of the HA/Tricalcium phosphate coating was  $28.26 \pm 0.28\mu\text{m}$ . The results confirmed the presence of HA, RGD and collagen on the CPTi surfaces. For the *in vitro* results the Collagen Group comparatively showed the most cells morphologically on the surface followed by the HA Group and Peptide Group on the 14<sup>th</sup> day of cell culturing respectively. For the MTT Assay, the ALP Assays and the Alizarin Red S., the Collagen Group showed comparatively and significantly better results than the other groups. The cell viability, proliferation, and mineralization significantly increased for the Collagen Group over the passage of time. **Conclusion:** In conclusion, collagen modified titanium surfaces yield a greater degree of osseointegration in comparison to RGD and HA coated surfaces. Collagen in conjunction with HA on CPTi surfaces can drastically enhance osseointegration *in vitro*. Collagen modified titanium surfaces yield a greater degree of osseointegration and produce more stable scaffolds on the implant surface when compared with RGD and HA/Tricalcium Phosphate coated CPTi surfaces *in vitro*.

## ABSTRAK

**Pengenalan:** Terdapat anjakan paradigma dalam implantology sejak kebelakangan ini. Dari implan yang klasik, dan tidak dapat berinteraksi dengan persekitaran mereka, kepada yang biomimetic dengan keupayaan untuk memberi kesan kepada persekitaran mereka. Implan dan lebih penting lagi, permukaan mereka, pada masa kini direka untuk meniru alam semula jadi. Oleh itu, tujuan kajian ini adalah untuk membandingkan sel morfologi, perkembangan dan pembezaan permukaan titanium dengan hydroxyapatite (HA) bersalut (biofunctionalized) dengan RGD dan collagen. **Objektif:** Objektif pertama kajian ini adalah untuk mengubah suai permukaan implan melalui “gritting”, pembagasan pasir, dan punaran asid permukaan titanium tulen (CPTi) supaya ia setanding dengan permukaan implan gigi yang boleh didapati secara komersial. Objektif kedua adalah untuk kot permukaan diubahsuai dengan HA menggunakan penyelesaian fluid simulasi badan (SBF) supaya lapisan seragam HA terbentuk di atas sampel. Objektif ketiga adalah untuk menggunakan penjerapan fizikal untuk “functionalizing” RGD dan kolagen pada permukaan CPTi HA/trikalsium fosfat. Objektif terakhir adalah untuk menggunakan HA/trikalsium fosfat sebagai kawalan untuk membandingkan sambutan *in vitro* ke atas sampel menggunakan osteoblas manusia. **Kaedah:** Terdapat tiga fasa untuk eksperimen ini, iaitu, fasa pengubahsuaian permukaan melalui “gritting”, pembagasan pasir, dan punaran asid. Fasa “functionalization” permukaan, di mana sampel CPTi disalut dengan hydroxyapatite (HA) dengan cecair badan simulasi (SBF), RGD dan kolagen. Fasa terakhir adalah fasa di mana *in vitro* morfologi sel, daya maju sel, percambahan sel dan mineral telah dinilai menggunakan sel osteoblast manusia (HOB) bagi tiga kumpulan yang berbeza daripada lapisan permukaan. **Keputusan dan Perbincangan:** Sampel sandblasted menunjukkan nilai kekasaran purata (Sa)  $2.48 \pm 0.74 \mu\text{m}$ . Sampel asid-terukir dipaparkan kekasaran yang lebih besar daripada sampel sandblasted dan gritted, iaitu, purata Sa sebanyak  $2.35 \pm 0.18 \mu\text{m}$ . Dalam

HA/trikalsium fosfat bersalut sampel, terdapat peningkatan umum dalam  $Sa$  dalam semua permukaan yang terlibat. Fosfat lapisan HA/trikalsium pada hari ke-14 menunjukkan purata nilai  $Sa$   $2.74 \pm 0.28\mu\text{m}$ . Ketebalan purata salutan HA/trikalsium fosfat adalah  $28.26 \pm 0.28\mu\text{m}$ . Keputusan mengesahkan kehadiran HA, RGD dan kolagen pada permukaan CPTi. Bagi analisis *in vitro* keputusan kumpulan kolagen menunjukkan sel-sel yang paling morfologi di permukaan diikuti oleh kumpulan HA dan peptide pada hari ke-14 pengkulturan sel masing-masing. Bagi MTT Assay, ALP Assays dan Alizarin Red S., kumpulan kolagen menunjukkan hasil yang agak jauh lebih baik daripada kumpulan-kumpulan lain. Sel daya maju, perkembangan, dan mineral meningkat dengan ketara bagi kumpulan kolagen lebih peredaran masa. Kesimpulan: Kesimpulannya, kolagen diubahsuai permukaan titanium menghasilkan tahap yang lebih tinggi untuk “osseointegration” berbanding dengan RGD dan permukaan bersalut HA. Kolagen dengan HA pada permukaan CPTi secara drastik boleh meningkatkan “osseointegration” *in vitro*. Kolagen mengubahsuai permukaan titanium menghasilkan tahap “osseointegration” yang lebih tinggi dan menghasilkan perancah lebih stabil di permukaan implan berbanding bersalut RGD dan HA/Trikalsium fosfat CPTi permukaan *in vitro*.

## ACKNOWLEDGEMENTS

I start with a quote that I think will be pertinent to the acknowledgements section of this thesis: “A teacher affects eternity; he can never tell where his influence stops.” - Henry Adams

Therefore, I would like to thank my teachers Dr. Muralithran G. Kutty and Prof. Dasan Swaminathan for believing in me and giving me an opportunity to work with them at Faculty of Dentistry, University Malaya. Their dedication and pursuit in achieving quality research has helped me grow both personally and professionally. Their research integrity and systematic approach to conduct research has been truly inspirational for me.

I specially thank Dr. Muralithran for allowing me to express my ideas and supporting me in various ways and advising me patiently during my ambitious endeavors in research. I also thank my wonderful colleagues, scientific officers, and friends that I have made along the way who have made my journey worthwhile.

My deepest appreciation and love goes towards my family and friends who have been there for me throughout the years. My parents have been sources of motivation for me and I have learnt from them each day how to become a better man. Hence, I dedicate this thesis to them, in yet another effort to prove myself worthy of their unconditional love.

## TABLE OF CONTENTS

ORIGINAL LITERARY WORK DECLARATION .....	2
ABSTRACT .....	3
ABSTRAK .....	5
ACKNOWLEDGEMENTS.....	7
LIST OF FIGURES .....	11
LIST OF TABLES .....	13
LIST OF SYMBOLS AND ABBREVIATIONS .....	14
LIST OF APPENDICES .....	16
<b>CHAPTER 1 – INTRODUCTION</b> .....	17
1.1. <i>Aim Of This Study</i> .....	19
1.2. <i>Objectives Of The Study</i> .....	20
1.3. <i>Null Hypothesis</i> .....	20
<b>CHAPTER 2 – LITERATURE REVIEW</b> .....	21
<b>2.1. Osseointegration</b> .....	21
2.1.1. <i>Surgery And Wound Healing</i> .....	21
2.1.2. <i>Osteoblasts And Bone Formation</i> .....	23
<b>2.2. Influence Of Implant Surface Topography On Osseointegration</b> .....	24
2.2.1. <i>Surface Roughness</i> .....	26
2.2.2. <i>Dual Acid-Etched Technique for Sandblasted and Acid-etched (SLA) Implants</i> .....	29
<b>2.3 Biomimetic Coatings</b> .....	30
2.3.1. <i>Hydroxyapatite Coated Implants</i> .....	30
2.3.2. <i>Collagen</i> .....	32
2.3.3. <i>Collagen And HA Composites As Implant Surface Coatings</i> .....	34
2.3.4. <i>Peptides</i> .....	35
2.3.3. <i>RGD And HA Composites As Implant Surface Coatings</i> .....	35
<b>2.4 Research Knowledge Gap And Motivation</b> .....	36
<b>CHAPTER 3 – METHODOLOGY</b> .....	37
<b>3.1. Research Methodology - Conceptual Framework</b> .....	37
<b>3.2. Surface Standardization and Modification</b> .....	38
3.2.1. <i>Gritting</i> .....	38
3.2.2. <i>Sandblasting</i> .....	39
3.2.3. <i>Acid Etching</i> .....	40

3.2.4. Activation of CPTi Surface With The Hydroxyl Group.....	41
<b>3.3. Surface Characterization .....</b>	<b>41</b>
3.3.1. HA Coating - Simulated Body Fluid (SBF) .....	41
3.3.2. Surface Analysis Of HA Coated Samples .....	44
3.3.3. HA Coated Samples Divided Into Randomly Selected Groups. ....	44
3.3.4. HA/Tricalciumphosphate Compound Incorporated With RGD .....	45
3.3.5. HA/Tricalciumphosphate Compound Incorporated With Collagen.....	46
<b>3.4. In Vitro Cell Study.....</b>	<b>47</b>
3.4.1. Coated Titanium Substrates And Their In Vitro Cell Response .....	47
3.4.2. Cell Morphology.....	48
3.4.3. Cell Viability And Proliferation .....	48
3.4.4. Cell Differentiation.....	49
3.4.5. Alizarin Red S. Staining - Detection of Calcium Deposits (Mineralization).....	50
3.4.6. Statistical Analysis .....	51
<b>CHAPTER 4 – RESULTS.....</b>	<b>52</b>
<b>4.1. Surface Modifications .....</b>	<b>52</b>
4.1.1. SEM Analysis Of Acid Etched Surfaces .....	52
4.1.2. Average Roughness Results Of Surface Modifications .....	53
<b>4.2 Surface Characterization .....</b>	<b>55</b>
4.2.1. Biomimetic HA Coating Morphology.....	55
4.2.2. HA Coating Thickness .....	57
4.2.3. The FTIR Results .....	58
4.2.4. EDS results of HA/Tricalcium phosphate Coated Samples .....	59
4.2.5. RGD Incorporated HA Coating Morphology.....	60
4.2.6. Collagen Incorporated HA Coating Morphology .....	61
4.2.7. EDS of RGD and Collagen Groups.....	63
<b>4.3 The In Vitro Results .....</b>	<b>64</b>
4.3.1. Cell Morphology - SEM Analysis .....	64
4.3.2. MTT Assay – Cell Viability Results .....	71
4.3.3. ALP Assay Results .....	73
4.3.4. Alizarin Red Staining - Detection of Calcium Deposits (Mineralization).....	74
<b>CHAPTER 5 – DISCUSSION.....</b>	<b>76</b>
<b>5.1 Surface Modifications .....</b>	<b>76</b>
<b>5.2 Surface Characterization .....</b>	<b>77</b>

5.2.1 SBF – HA Coating .....	77
5.2.2. Collagen Type I Coating .....	79
5.2.3. RGD Coating .....	80
<b>5.3 In Vitro Cell Response</b> .....	<b>81</b>
5.3.1 Cell Viability.....	81
5.3.2. Cell Differentiation.....	82
5.3.3. Mineralization .....	83
5.3.4. Limitations Of The Study .....	83
5.3.5. Recommendations For Future Studies .....	84
<b>CHAPTER 6 – CONCLUSION</b> .....	<b>84</b>
<b>SUPPLEMENTARY</b> .....	<b>96</b>
<i>Publication and Conferences</i> .....	96
<b>APPENDIX</b> .....	<b>97</b>
<i>Appendix A - Raw Sa Data</i> .....	97
<i>Appendix B - Raw MTT Assay Data</i> .....	101
<i>Appendix C – Raw ALP Data</i> .....	103
<i>Appendix D – Raw SPSS Data</i> .....	104
<i>Surface Modifications – Raw Data</i> .....	104
<i>MTT Assay – Raw Data</i> .....	109

## LIST OF FIGURES

1. *Figure 1*: Shows a summarized flowchart of the conceptual framework of the methodology that was undertaken.
2. *Figure 2*: Twin variable grinding and polishing machine (250 High Speed Twin Grinder-Polisher by Buehler) was used for gritting the CPTi surfaces.
3. *Figure 3*: Shows the sandblasting machine (SB-8060-KP Techno Finishing Sdn. Bhd. Malaysia.) used for this study.
4. *Figure 4*: Shows a flowchart of how the samples were divided into three groups.
5. *Figure 5A & 5B*: Show the SEM image of Acid-Etched samples at 1000x and 10,000x magnification with a voltage of 10 kV and a Working Distance (WD) of 10mm.
6. *Figure 6*: Shows a graphical representation of the average  $Sa$  values obtained for each sample.
7. *Figure 7*: Shows a graphical representation of the overall  $Sa$  values obtained for all the samples.
8. *Figures 8A & 8B*: Show 7<sup>th</sup> day samples. *Figures 8C & 8D* show 14<sup>th</sup> day samples under the SEM containing HA/Tricalcium phosphate coating at 10,000x and 20,000x magnification respectively.
9. *Figures 9A and 9B*: Show the thickness of the samples on the 14<sup>th</sup> day of Tas-SBF immersion.
10. *Figure 10*: Shows the FTIR of the surface coatings after 14days of TAS-SBF immersion.
11. *Figures 11A & 11*: Show the EDS elemental analysis of CPTi surfaces coated with HA/Tricalcium phosphate on the 7<sup>th</sup> and 14<sup>th</sup> day.
12. *Figures 12A and 12B*: Show freeze dried Peptide Group samples at a magnification of 20,000x & 60,000x at a voltage of 10 kV and a Working Distance (WD) of 10mm under the SEM.

13. *Figures 13A and 13B:* Show freeze dried Collagen Group samples at a magnification of 10,000x & 20,000x at a voltage of 10 kV and a Working Distance (WD) of 10mm under the SEM.
14. *Figures 14A & 14B:* Show the EDS elemental analysis of the RGD Group and the Collagen Group respectively.
15. *Figures 15 A-C:* Show the cell morphology of the HA Group on the 7<sup>th</sup> Day. *Figures 15 D-F:* Show the cell morphology of the Peptide Group on the 7<sup>th</sup> Day. *Figures 15 G-I:* Show the cell morphology of the Collagen Group on the 7<sup>th</sup> Day.
16. *Figures 16 A-C:* Show the cell morphology of the HA Group on the 14<sup>th</sup> Day. *Figures 16 D-F:* Show the cell morphology of the Peptide Group on the 14<sup>th</sup> Day. *Figures 16 G-I:* Show the cell morphology of the Collagen Group on the 14<sup>th</sup> Day.
17. *Figure 17:* Shows the descriptive average MTT Assay results graphically.
18. *Figure 18:* Show a bar chart of the average values of the ALP Assay.
19. *Figures 19 A-B:* Show the mineralization of the HA Group samples on the 14<sup>th</sup> Day. *Figures 19 C-D:* Show the mineralization of the Peptide Group on the 14<sup>th</sup> Day. *Figures 19 E-F:* Show the mineralization of the Collagen Group on the 14<sup>th</sup> Day.

## LIST OF TABLES

1. *Table 1:* Order and quantity of chemical reagents supplied by Sigma Aldrich Sdn. Bhd mixed to prepare Tas-SBF solution.
2. *Table 2:* Shows significant difference amongst the various groups.
3. *Table 3:* Shows the parametric ANOVA test to analyze the variance between the types of coatings on each day of the MTT Assay analysis.
4. *Table 4:* Shows the parametric ANOVA results for each of the three groups for the MTT Assay.
5. *Tables 5:* Shows the results of the ALP Assay on days 7 and 14 respectively.

University of Malaya

## LIST OF SYMBOLS AND ABBREVIATIONS

This list of abbreviations is arranged in an alphabetical order.

AE	–	Acid Etch
ALP	–	Alkaline Phosphatase
ANOVA	–	One-Way Analysis of the Variance
BIC	–	Bone-to-Implant Contact
BMPs	–	Bone Morphogenetic Proteins
CaP	–	Calcium Phosphate
CPTi	–	Commercially Pure Titanium
DMEM	–	Dulbecco's Modified Eagle's Medium
EDS	–	Energy-dispersive X-ray Spectroscopy
EDTA	–	Ethylenediaminetetraacetic Acid
FBS	–	Fetal Bovine Serum
FGF	–	Fibroblast Growth Factor
FTIR	–	Fourier Transform Infrared Spectrometer
HA	–	Hydroxyapatite
HOB	–	Human Osteoblasts
MTT	–	3-[4,5-dimethylthiazol-2-yl]-2,5-diphenyltetrazolium Bromide
MUP	–	Methylumbelliferyl Phosphate Disodium Salt
PHSA	–	Plasma Sprayed Hydroxyapatite
RGD	–	Arginine-Glycine-Aspartate
<i>Sa</i>	–	Average Roughness

SB	–	Sandblast
SBF	–	Simulated Body Fluid
Tas-SBF	–	Simulated Body Fluid (according to the work of Jalota <i>et al.</i> 2006)
SEM	–	Scanning Electron Microscope
SLA	–	Sandblasted And Acid Etched Surface
SPSS	–	The Statistical Package for the Social Sciences
WD	–	Working Distance

University of Malaya

## **LIST OF APPENDICES**

1. Appendix A - Raw Sa Data
2. Appendix B - Raw MTT Assay Data
3. Appendix C – Raw ALP Data
4. Appendix D – Raw SPSS Data

Surface Modifications – Raw Data

MTT Assay – Raw Data

University of Malaya

## CHAPTER 1 – INTRODUCTION

Ample stresses and strains can be afflicted onto the bone to cause a fracture when it is subjected to trauma or surgery (Dimitriou *et al.*, 2005). A complex series of healing processes occur after the bone tissue is subjected to such a fracture. These healing pathways also come into play after a dental implant is inserted into its nesting site. In implant therapy, this is termed as osseointegration (Albrektsson *et al.*, 1981). In cases where the body cannot restore normal function, implantation is required to necessitate the functional requirements of the missing tissue. Implants can be temporary and permanent. Osseointegration is an attribute of permanent endosseous implant therapy and its successful stepwise completion is of paramount importance. It enables the implant to directly contact the newly formed bone after surgery and withstand the functional loads that are imposed onto it over extended periods of time (Branemark, 1983). Since the 1980s, there have been numerous studies which have proven that the implant material is limited in providing biocompatibility. It is actually the nature of the surface of the implant that dictates the fundamental influence of the implant on the surrounding tissue (Le Guéhennec *et al.*, 2007).

Titanium has played a big role in implantology because it possesses favorable bulk properties and its surface suits the functional requirements that an implant ought to inculcate. An added advantage of using titanium as an implant material, amongst many, is that once osseointegration occurs, the implant has a high capacity to bear various functional loads. Titanium is an inert material because it possesses a passive titanium dioxide layer on top which protects the implant from being degraded by the adverse healing conditions and environments that it is subjected to. This helps the implant last longer without the need for replacement. Also, when the host response is assessed, the passive titanium dioxide layer helps in chemically stabilizing the implant so that inflammation and fibrous tissue formation is prevented. This ensures eventual physical stability of the implant too (Albrektsson *et al.*, 1981).

Along with the proper choice of bulk material, latest research focuses on making titanium implants that promote bone growth and regeneration (Kämmerer *et al.*, 2016). One of the ways of achieving more successful implant therapy is to use natural or synthetic materials on the surface on the implants. This is called the biomimetic way of enhancing implant design and it employs nature as its guide. Researchers have modified the surfaces of implants and it has been shown to fasten healing and increase bone growth. Nowadays, implant design and the effects of varying surface topographies and compositions are topics of leading implant researches (Cho *et al.*, 2016).

There is a paradigm shift in implantology in recent times. From implants being classically inert, and unable to interact with their environment, to them being biomimetic with the ability to affect their surroundings. Implants and more importantly their surfaces, are nowadays designed to mimic natural biological materials (Tenget *et al.*, 2016).

There are certain methods that have been invented and researched upon to promote osseointegration, we can divide them into inorganic and organic. The inorganic procedure of modifying a surface is to use particular topographies and alter the chemical composition of the implant. Some of these inorganic alterations to the implant surface have proven successful in promoting implant to bone contact, primary stability of the implant, and eventually osseointegration (Tao *et al.*, 2016).

A stage ahead of inorganically altering the implant is to “biofunctionalize” it. This is the organic way of modifying a surface through biochemical functionalization of the surface of the implant. The organic constituents of the extracellular matrix are used to mimic the microenvironment of the cell at certain times in the fracture healing phase of implant therapy. The otherwise inert titanium implant is

rendered bioactive and can consequentially be a source of proteins and peptides that promote different phases of osseointegration (Raphel *et al.*, 2016).

Inorganically the bone is made up of hydroxyapatite (HA). Organically, the commonest protein in the bone is collagen type I and the functional component of a lot of extracellular proteins is a peptide called RGD (Arginine-Glycine-Aspartate) (Raphel *et al.*, 2016). There have been studies that individually compare the successful *in vitro* effects of biofunctionalized surfaces with hydroxyapatite (HA), Collagen, and RGD (Rammelt *et al.*, 2006; Raphel *et al.*, 2016; Tao *et al.*, 2016). There have been a few studies that use these individual components together to biofunctionalize implant surfaces but we are not aware of any studies that compare their *in vitro* effects between each other.

### *1.1. Aim Of This Study*

The aim of this study was to compare the cell morphology, proliferation and differentiation of titanium surfaces biofunctionalized and characterized by HA/Tricalcium phosphate, RGD, and Collagen.

### *1.2. Objectives Of The Study*

1. The first objective of the study was to modify the surface of the implant by gritting, sandblasting, and acid-etching the CPTi surfaces so that they are comparable to the commercially available implant surfaces.

2. The second objective was to coat the modified surfaces with HA/Tricalcium Phosphate using a Simulated Body Fluid (SBF) solution so that a uniform layer of HA is formed on top of the samples.
3. The third objective was to use physical adsorption for functionalizing RGD and Collagen on the HA/Tricalcium Phosphate coated CPTi surfaces.
4. The final objective was to use the HA/Tricalcium Phosphate as the control to compare the *in vitro* response on the samples using human osteoblasts.

### *1.3. Null Hypothesis*

RGD AND Collagen modified titanium surfaces do not yield a greater degree of osseointegration and do not produce more stable scaffolds on the implant surface when compared with HA/Tricalcium Phosphate coated CPTi surfaces *in vitro*.

## CHAPTER 2 – LITERATURE REVIEW

Studies that investigate the *in vitro* biofunctionalization of titanium implants hold the ultimate goal of achieving better osseointegration. Hence this literature review section outlines various steps of osseointegration and eventually discusses the inorganic and organic ways of making osseointegration better in terms of enhancing the surface properties so that the host response can be favourable.

### 2.1. Osseointegration

#### 2.1.1. Surgery And Wound Healing

Wound healing around a dental implant placed into a prepared osteotomy (the surgical cutting of a bone or removal of a piece of bone.) follows three stages of repair: Initial formation of a blood clot occurs through a biochemical activation followed by a cellular activation and finally a cellular response (Stanford, 2010). During surgery, dental implant surfaces interact with blood components from ruptured blood vessels. Within a short period of time, various plasma proteins such as fibrin get adsorbed on the material surface. Fibrinogen is converted to fibrin and hence the complement and kinin systems are activated (Bateman & Carr, 2008). As it occurs in fracture healing, the migration of bone cells in peri-implant healing occurs through the fibrin of a blood clot. Since fibrin has the potential to adhere to almost all surfaces, it can be anticipated that the migration of osteogenic cell populations towards the implant surface will occur too. However, as the migration of cells through fibrin causes retraction of the fibrin scaffold, the ability of an implant surface to retain this fibrin scaffold during the phase of wound contraction is critical in determining whether the migrating cells will reach the implant surface or not.

The activation of platelets occurs as a result of interaction of platelets with the implant surface as well as the fibrin scaffold and this leads to a thrombus formation and blood clotting (Bateman & Carr, 2008). Moreover, platelets are a rich source of many growth and differentiation factors which play a key role in the wound healing process by acting as signalling molecules for the recruitment and differentiation of undifferentiated mesenchymal stem cells at the implant surface. Plasma also contains dissolved substances such as glucose, amino acids, various ions, cholesterol, and hormones which are needed to preserve the integrity of cells and tissues (Anderson & Anderson, 2002).

Blood is the first tissue to come into contact with the implant. This leads to protein adsorption, which is dependent on the surface properties of the implant. Hydrophilic surfaces perform better in these adverse healing processes hence newer dental implants have been developed with highly hydrophilic and relatively rough surfaces which exhibit better osseointegration than conventional dental implants. Adsorption of proteins such as fibronectin and vitronectin on the surface of dental implants may enhance cell adhesion and osseointegration (Albrektsson *et al.*, 2001).

In the beginning of implant therapy, various immune cells govern the tissue response. This is soon superseded by the migration of phagocyte macrophages to the implantation site which remove the necrotic debris left by the surgical process. These cells then undergo physiological changes that induce the expression of cell surface proteins while the production of cytokines and pro-inflammatory mediators takes place as well (Albrektsson & Johansson, 2001). Macrophages can affect cellular recruitment, migration, proliferation and formation of an extracellular matrix on the implant surface. They express growth factors such as: fibroblast growth factors (FGF-1, FGF-2, and FGF-4), transforming growth factors, epithelial growth factors as well as bone morphogenetic proteins (BMPs). Consequently, angiogenesis takes place in the implantation site because of all this activity.

Angiogenesis is the process of creation of new blood vessels that replace those affected by trauma. It is a fundamental step in new bone formation and bone-implant integration, because the cells associated with osteogenesis, namely the osteoblasts, are unable to survive and create new bone if they are not surrounded by blood vessels (Terheyden *et al.*, 2012).

Before the formation of bone adjacent to the implant surface, an extracellular matrix needs to be formed. For this to happen, fibroblasts attach to integrin binding sites of cell-adhesive molecules such as fibronectin that has already been adsorbed onto the implant surface at this point and begin the formation of granulated tissue (Friedl & Brocker, 2000). Growth factors are chemotactic for fibroblasts and induce their differentiation and production of extracellular matrix proteins (Anitua *et al.*, 2012).

### 2.1.2. Osteoblasts And Bone Formation

Osteoblasts are introduced to the implant surface and adhere via the integrin binding sites of the pre-adsorbed protein layer. The composition of this pre-adsorbed layer and of the provisional matrix formed at the vicinity of the implant surface is crucial to modulate the chemo attraction and differentiation of osteoprogenitor cells into osteoblasts. Once attached to the implant surface, osteoblasts begin secreting the extracellular matrix and express alkaline phosphatase and osteocalcin. Osteoblasts secrete collagens to form a primary matrix of either type II in endochondral ossification or type III in intramembranous ossification, but which in both cases ends up replaced by collagen type I. Primary bone formation is rather rapid: mineralization is mostly extrafibrillar with respect to collagen, giving rise to an unorganized bone structure called woven bone that grows from the implant surface to fuse with the mineralizing front of the host bone (Davies, 2003). During this process, some

of the fully differentiated osteoblasts in charge of the mineralization are trapped within circular grooves called lacunae and become osteocytes. This structure is particular of the immature woven bone. Woven bone serves to stabilize the fractured tissue and the implant within the implantation site by filling the grooves of the implant threads. Consequently, woven bone is rapidly replaced during the process of remodelling. At the site of implantation, far from the implant surface, remodelling takes place in the host bone from the very beginning of trauma and extends for several months (Brunski, 1999). Therefore, remodelling takes place first within the host bone and then within the woven bone that forms at the implant surface. Remodelling is the basic regulatory process of bone and implies the close interplay of the bone cells, osteoclasts and osteoblasts, regulated by osteocytes and a series of different signalling pathways and molecules. It is consequentially the last stage in the process of osteogenesis around implants but is a continuous process in the life of all mature bones (De Arriba *et al.*, 2016).

## **2.2. Influence Of Implant Surface Topography On Osseointegration**

Dental implant quality depends on the chemical, physical, mechanical, and topographic characteristics of the implant surface (Grassi *et al.*, 2006). These different properties interact and determine the activities of the attached cells that are close to the dental implant surface. Dental implants have been designed to provide textures and shapes that may enhance cellular activity and direct bone apposition (Huang *et al.*, 2005). Osteogenesis at the implant surface is influenced by several mechanisms. A series of coordinated events, including cell proliferation, transformation of osteoblasts and bone tissue formation might be affected by different surface topographies (Shibli *et al.*, 2007). The amount of bone-to-implant contact (BIC) is an important determinant in long-term

success of dental implants. Hence, maximizing the BIC through surface roughness of the implant has become a goal of implant therapy (Soskolne *et al.*, 2002).

Albrektsson *et al.* (1981) recognized that among the factors influencing BIC such as topography, chemistry, wettability and surface energy the most important is wettability. Surface wettability is largely dependent on surface energy and influences the degree of contact with the physiological environment (Kilpadi & Lemons, 1994, Zhao *et al.*, 2005). Several evaluations have demonstrated that implants with rough surfaces show better bone apposition and BIC than implants with smooth surfaces (Buser *et al.*, 1999, Cochran *et al.*, 2002). Surface roughness also has a positive influence on cell migration and proliferation, which in turn leads to better BIC results, suggesting that the microstructure of the implant influences biomaterial–tissue interaction (Matsuo *et al.*, 1999, Novaes *et al.*, 2002). Implant surface properties are likely to be of particular relevance to the chemical and biological interface processes in the early healing stages after implantation. It is generally accepted that these early stages are likely to have an effect on the host response to the implant and, therefore, the long-term outcome and success of the treatment.

Surface chemistry has the potential to alter ionic interactions, protein adsorption and cellular activity at the implant surface (Schliephake *et al.*, 2005). These modifications may subsequently influence conformational changes in the structures and interactive natures of adsorbed proteins and cells. Modifications to the implant surface chemistry may lead to alterations in the structure of adsorbed proteins and have cascading effects that may ultimately be evident at the clinical level. In vivo evidence has supported the use of alterations in surface chemistry to modify osseointegration events. Specifically, an investigation utilizing sandblasted, large-grit, and SLA (Sandblasted and Acid Etched) surfaces that were chemically different but had the same physical properties was conducted

to assess BIC as a measure of osseointegration. The chemically enhanced SLA surface demonstrated significantly enhanced BIC during the first 4 weeks of bone healing, with 60% more bone than the standard SLA surface after 2 weeks (Buser *et al.*, 2004). The chemical modifications for the test SLA surface resulted in increased wettability i.e. in a hydrophilic surface rather than a hydrophobic one. Water contact angles of zero degrees were seen with the chemically enhanced surface compared to 139.9 degrees for a standard SLA surface, and this hydrophilicity was maintained after drying (Rupp *et al.*, 2006).

### 2.2.1. Surface Roughness

A detailed description of the processes most widely employed for obtaining micron-sized roughness and micro-waviness on titanium implant surfaces shall be described in this literature. The relevant methods are sandblasting (SB), acid etching (AE), and spark anodization or oxidation (Ox).

SB stands for the projection of abrasive particles usually  $\text{Al}_2\text{O}_3$ ,  $\text{TiO}_2$ ,  $\text{SiO}_2$  or HAP, under high pressure at a certain object to attain a certain degree of surface roughness. The impact of these particles with a titanium surface scrapes off the top layer of the substrate and creates craters of plastic deformation on the impacted spots. The degree of deformation depends upon the projected particle composition, size, nature and history of the target surface (Wennerberget *et al.*, 1996).

Sandblasting can result in anisotropic surface characteristics depending on the time of exposure and positioning of the sample with respect to the particle jet. After sandblasting, a number of the projected particles remain embedded on the substrate surface and this alters its chemical properties (Marinho *et al.*, 2003). This substrate heterogeneity has been reported to reduce the corrosion resistance and

even impair cell function and mineralization (Piattelliet *al.*, 1996). Therefore, nowadays the most used sandblasted protocols include an acid etching post-cleaning step that contributes to dissolve at least some of the projected particles (D. Cochran *et al.*, 1998; Roehlinget *al.*, 2015).

AE is based on the selective dissolution of the substrate grains after dissolution of the native oxide layer. Usually, the AE process produces craters an order of magnitude smaller than those produced by sandblasting. This has been exploited to produce multidimensional micron-sized surfaces of roughness varying between 0.2 and 2 $\mu\text{m}$  (Tejero *et al.*, 2014). However, proper combinations of substrate grain distribution and AE recipes may lead to similar levels of roughness without need of previous sandblasting steps. Factors affecting AE outcomes include the acids employed, the time of exposure and the temperature. But most importantly, a detailed knowledge of the substrate properties is of paramount importance to obtain the desired results in a reproducible manner.

Another method to obtain micron-sized roughness consists of applying an electrical voltage through a conducting acid or base electrolyte solution and above the electrical breakdown level of the oxide layer. In these conditions, sparking occurs and violent morphological changes on the substrate surface ensue. The incorporation of ions from the electrolyte and subsequent growth of the oxide layers also takes place below the breakdown voltage, but in these cases no significant changes in the surface topography follow. For a given material and electrolyte couple, there is a voltage threshold (breakdown voltage) that separates anodizing from spark anodizing. These processes are often named as oxidizing or anodic oxidation (Banakh *et al.*, 2016).

However, in recent times, the commonest technique used to achieve surface roughness in dental implants is a combination of SB, followed by AE. This combination produces both micro-roughness

and waviness which significantly increases early endosseous integration, peri-implant bone healing and the stability of the implant (Novaes Jr *et al.*, 2010).

Surface roughness plays a key role in osseointegration (Le Guéhennec *et al.*, 2007). Various in vitro and in vivo studies have proven that surface roughness effects osteoblastic spreading and proliferation, differentiation, and protein synthesis (Sammons *et al.*, 2005; Zhao *et al.*, 2006). When dimensionally measured, surface roughness can be categorized into: macro-roughness, micro-roughness and nano-roughness.

Macro roughness of implants comprises of features in the range of millimeters to tens of microns. This directly relates to implant geometry, with threaded screw and macro porous surface treatments. Primary implant fixation and long-term mechanical stability can be improved by an appropriate macro roughness (Shalabi *et al.*, 2006; Wennerberg *et al.*, 1996).

Micro roughness in orthopaedic and dental implants is defined as being in the range of 1–10 $\mu$ m. This range of roughness maximizes the interlocking between mineralized bone and implant surface. Clinical studies suggest that the micron-level surface roughness results in greater success of implants (Junker *et al.*, 2009; Shalabi *et al.*, 2006).

Nanotechnology involves materials that have a nano-sized topography or are composed of nano-sized materials with a size range between 1 and 100 nm. Nanometer roughness plays an important role in the adsorption of proteins, adhesion of osteoblastic cells and thus the rate of osseointegration (Brett *et al.*, 2004).

### 2.2.2. Dual Acid-Etched Technique for Sandblasted and Acid-etched (SLA) Implants

There are many different acid combinations and methods to achieve a proper roughened surface (Tejero *et al.*, 2014). One successful technique incorporates the immersion of titanium implants for several minutes in a mixture of concentrated HCl and H<sub>2</sub>SO<sub>4</sub> heated above 100 °C. This is called dual acid-etching and is employed to produce a micro-rough surface. These surfaces enhance the osteoconductive process through the attachment of fibrin and osteogenic cells, resulting in bone formation directly on the surface of the implant (Park & Davies, 2000).

This technique of acid etching produces higher adhesion and expression of platelets and extracellular genes, therefore helping in colonization of osteoblasts. Various studies confirm that surfaces produced with this style of acid etching show higher BIC and lower rates of bone resorption when compared with other conventional surfaces (D. Cochran *et al.*, 1998; D. L. Cochran *et al.*, 2002). The wettability of the surface has also been shown to increase fibrin adhesion. This provides contact guidance for the osteoblasts migrating along the surface of the implant (Buser *et al.*, 2004). If an implant surface is sandblasted and consequently dual acid-etched, it can be termed as a SLA surface. This type of surface is produced by a large grit 250-500µm blasting process followed by acid-etching. Sandblasting results in surface roughness and acid etching leads to micro-texture and debris removal. Implant surfaces that undergo these procedures are known to have increased bone integration (Bornstein *et al.*, 2008; Hotchkiss *et al.*, 2016).

## 2.3 Biomimetic Coatings

Latest research suggests the application of various biomimetic coatings can be beneficial for implant therapy success (Kulkarni *et al.*, 2014; Preshaw, 2015). The human bone inherently embodies HA (Liao *et al.*, 2006). A significant mineral portion of the bone is composed of these nanometre sized Calcium Phosphate (CaP) crystals that measure up to about 5-20 nm in width and 60 nm in length. A cycle of osteoclastic and osteoblastic activity ensures that a certain haemostatic level of HA is maintained at all times in living bone (Ferrazet *et al.*, 2004). HA is a bioactive and biocompatible material and has been used rigorously in research and clinical settings in various shapes and forms (Suchanek & Yoshimura, 1998).

### 2.3.1. Hydroxyapatite Coated Implants

Titanium surfaces coated with HA ( $\text{Ca}_{10}(\text{PO}_4)_6(\text{OH})_2$ ) can be considered as bioactive because of a series of processes that result in precipitation of a CaP rich layer on the implant surface through a solid solution ion exchange at the implant bone interface (Ducheyne & Cuckler, 1992). Synthetically produced HA has been widely investigated due to the similar chemical composition to the natural mineral matrix of human bone (Ducheyne & Cuckler, 1992).

HA surface coatings on the titanium surfaces have proven osteoconductive properties (S.-W. Lee *et al.*, 2014). HA could influence protein interactions and consequently lead to favourable healing and greater osteoblast adhesion, proliferation and differentiation (Webster *et al.*, 2000). There is extensive literature that deals with the various procedures of acquiring HA coating on different surfaces. Amongst these methods, the wet chemical deposition, thermal plasma spraying, pulse laser deposition, the sol-gel, electrodeposition and biomimetic deposition are the ones that have been most verified and reported (Zakaria *et al.*, 2013).

Nowadays, 20–50µm thick Plasma Sprayed Hydroxyapatite (PSHA) coatings can be found on many commercial bio-ceramic coatings. These coatings usually depend upon mechanical interlocking with grit-blasted or acid etched metallic surfaces. It has been found that osseointegration of the dental implants with PSHA is faster than uncoated implants. Bone maturation has been shown to improve with HA coated implants too as compared to implants with more conventional surfaces (Knabe *et al.*, 2002).

Amid various techniques to coat implant surfaces with HA is the biomimetic deposition method in which a simulated body fluid (SBF) solution is prepared in accordance with the inorganic ingredients of the human blood plasma (Nazir *et al.*, 2015). The biomimetic approach exploits the advantageous consequences of using an SBF solution to coat the surface with HA. An HA layer on titanium surfaces using SBF is capable of achieving a crystallinity and morphology similar to that of a bone-like apatite (Gandolfi *et al.*, 2015). The fact that SBF creates apatite crystals that resemble human bone on titanium and other surfaces is testified by various literature (Al-Haddad *et al.*, 2015; Karamian *et al.*, 2002; Kokubo & Takadama, 2008). The ability of forming this apatite layer often determines the bonding ability of an implant material to adjacent living bone (Jonášová *et al.*, 2004). This bioactive deposition can stimulate bone apposition and the healing process. Hence, early osseointegration of titanium implants may be established (Chrcanovic *et al.*, 2012; Davies, 2003; Kokubo *et al.*, 1990; Lavenus *et al.*, 2010; Villar *et al.*, 2011). Generally, biomimetic coating processes are performed for about seven to fourteen days (Oscar *et al.*, 2015). There are some treatment methods however that temper with the concentration of SBF solutions and can considerably reduce the SBF immersion time and create favourable HA deposition (D. H. Yang *et al.*, 2015).

When SBF is used to coat HA on titanium surfaces, a wide range of therapeutic or biomimetic agents can be incorporated into the layer that forms on the titanium surface. This opens new doors into medicinally or biomimetically enhancing the implant surface ensuring a steady and controlled release of the surface constituents. Incorporating pharmacological and/or other ingredients with implant surfaces can be very clinically relevant in patients that lack adequate bone support. Bisphosphonates, simvastatin and various antibiotics are a few examples of what is being researched upon nowadays (Nazir *et al.*, 2015).

### 2.3.2. Collagen

In humans, collagen has 28 different varieties but osteoblasts only produce type I collagen. Approximately 90% of the bone is composed of collagen, while the rest constitutes of relatively soluble, non-collagenous proteins such as bone sialoproteins (BMPs), osteonectin, fibronectin, osteocalcin etc. (Geissler *et al.*, 2000).

The composition of Type I collagen consists of a polypeptide backbone that is helical in nature. This helical design houses roughly a thousand amino acids with 30% of them being glycine (Gly). Some uncommon residues are also found in collagen i.e. residues of Proline(Pro), Hidroxyproline (Hyp) and Hidroxylysine (Hyl) (Geissler *et al.*, 2000).

The structure of collagen is composed of 3 non-coaxial polypeptide chains with repeated fractions of three amino acids, namely and usually Gly-Pro-Hyp. This sequence recurs about 338 times along the chain. The chains organize themselves into tropocollagen, which forms cross-linkages with other similar chains and enhances stability. The organization of these is quarter-staggered. This allows

grooves to develop in the midst that act as areas of heterogeneous nucleation of calcium phosphate precursors. These nuclei mineralize and expand into hydroxyapatite nano-crystals (Ramachandran & Kartha, 1954).

Collagen has many roles and properties that are necessary in the human body. It acts as a template for bio-mineralization and possesses low antigenicity, inflammatory and cytotoxic responses. It also aids in mechanical stability and governs cell adhesion and migration. Plus, it is necessary for general tissue support for hemostasis and repair (Bailey & Robins, 1975).

In relation to osteogenesis, collagen helps bind osteoprogenitor cells via integrin receptors on the cell surface such as  $\alpha 2\beta 1$ ,  $\alpha V\beta 3$  and  $\alpha V\beta 5$  etc. Furthermore, like other extracellular proteins such as vitronectin, laminin and fibronectin, collagen is a useful exponent in cellular adhesion and spreading. This is because it has the peptide sequence arginine-glycine aspartic-acid (RGD) in its make-up. This arrangement of peptides in collagen helps in cell adhesion because it attaches specifically to the receptors of integrins (Hynes, 1992).

Cell adhesion has the effect of bringing about phosphorylation of the focal adhesion kinases. This consequentially activates intracellular transduction of biomolecules that alter cell functions and fate. Collagen is often utilized as a bone filling material in both dental and orthopedic fields because of its osteogenicity. Yet it is additionally the most enduring pro-coagulant structural protein in the sub-endothelium. It mingles with platelet membranes to bring about platelet adhesion, activation and helps discharge growth factors from platelets when there is vascular damage (Wahl & Czernuszka, 2006). Additionally, collagen can be remodeled to form three-dimensional scaffolds or implant surface coatings, which is useful in terms of making biomimetic implant surfaces.

Various studies have demonstrated the osteogenic potential of biomimetic implant surface collagen coatings (Ao *et al.*, 2016; Sartori *et al.*, 2015). Collagen is a complicated molecule that requires several pre-processing steps to transform into a functional coating. The structural attributes of the coatings require specific techniques to spread the coating onto the surface and to stabilize this formation by cross-linkages (Ao *et al.*, 2016).

### 2.3.3. Collagen And HA Composites As Implant Surface Coatings

Human bones comprise mainly of collagen type I and HA. Both of these materials have osteoconductive properties. Therefore, an implant made from either of these materials is most likely to act in a similar way. It has been shown that collagen type I and HA enhance osteoblast differentiation but when they are combined together, they show greater osteogenesis (Wahl *et al.*, 2006). These collagen and HA composites also performed better mechanically due to the ductile nature of collagen that aids in increasing the poor fracture toughness of HA. The addition of a CaP compound to collagen scaffolds gives greater stability, higher resistance to three-dimensional swelling and increased wettability (Wahl *et al.*, 2006). Therefore, combining collagen and HA should provide an edge over other materials for use in bone tissue repair.

### 2.3.4. Peptides

When osteogenic cells attach to proteins such as collagen and fibrin, there is an active peptide segment of these proteins that comes into play. These peptides possess a particular sequence of amino acids which helps integrins that exist along the membranes of cells to facilitate in cell attachment and

adhesion (Hynes, 2002). The attachment of cells triggers downstream signaling processes that further aid in cell migration, cell cycle progression and differentiation. Hence, one way of biofunctionalizing implants is to use the active amino acid sequences of proteins on the implant surfaces instead of the whole parent protein sequences.

The RGD amino acid sequence is the one that is often used to biofunctionalize surfaces. This is because of the biological impact it has on cell behavior. RGD was found by Pierschbacher and Rouslahti who termed it as the smallest necessary peptide sequence in fibronectin that promotes cell adhesion (Pierschbacher & Ruoslahti, 1984). Since then, cell adhesive sites of various matrix proteins such as vitronectin, fibrinogen, von Willebrand factor, laminin, and bone sialoprotein have been found and tested on surfaces to promote cell adhesion (Pfaff, 1997).

### 2.3.3. *RGD And HA Composites As Implant Surface Coatings*

There have been a lot of studies that have proven RGD as a useful tool to enhance cell adhesion on various materials (Hersel *et al.*, 2003). There have been a few studies that have shown the effect of RGD in conjunction with HA on a surface to enhance the cellular response (C. Yang *et al.*, 2009). Collectively, the results suggest a potential therapeutic benefit for functionalizing HA with RGD (Sawyer *et al.*, 2005).

## **2.4 Research Knowledge Gap And Motivation**

Individually and collectively there have been studies that test the *in vitro* cell response of RGD, Collagen and HA but there have been a few studies that use these individual components together to biofunctionalize implant surfaces. We are not aware of any studies that compare the *in vitro* effects of HA with HA modified Collagen and RGD composites on CPTi surfaces using the Tas-SBF and physical adsorption methods for coating. This study shall pave way into making it possible for implant surfaces be one step closer at achieving greater osseointegrative success.

University of Malaya

## CHAPTER 3 – METHODOLOGY

### 3.1. Research Methodology - Conceptual Framework

This study was done to establish if the surface coatings of the composites of HA/RGD and HA/Collagen perform better *in vitro* than a HA coating alone. *Figure 1* shows a conceptual framework of the methodology that was undertaken to prove the hypothesis that initiated this research. There were three phases to this experiment, namely, the surface modification phase where gritting, sandblasting, and acid etching took place. The surface characterization phase, where the CPTi samples were coated with HA, RGD and collagen. The last phase was the *in vitro* phase where cell response was assessed for the three different groups of surface coatings.

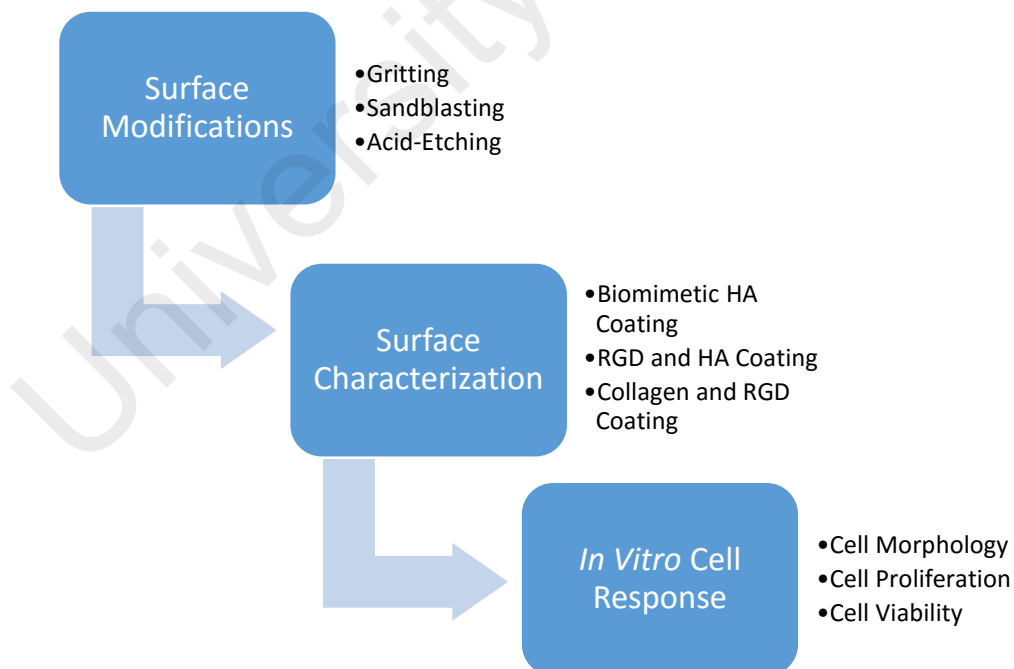


*Figure 1*: Shows a summarized flowchart of the conceptual framework of the methodology that was undertaken.

### 3.2. Surface Standardization and Modification.

For this study, commercially pure grade 2 titanium (CPTi) discs from E-Steel Sdn. Bhd. (Selangor, Malaysia) were used. The discs were cut square in shape and measured 10mm × 10 mm. An EDM wire cutter (CNC Wirecut Sodick A500, MARK 21) was used to cut the CPTi sheets into the desired dimensions. Before starting the experiment, the discs had to be standardized by gritting.

#### 3.2.1. Gritting.

Silicon carbide papers with 400, 600, 800, 1000, and 1200 grit were used for sequentially gritting or polishing and hence standardizing the titanium substrates by using a twin variable speed grinding and polishing machine (250 High Speed Twin Grinder-Polisher by Buehler) for two minutes at each specific grit at 300 rpm as seen in *Figure 1*. This process ensured that all samples possessed similar roughness to each other before the beginning of the study.

An Alicona Infinite Focus Optical 3D Measurement Device G4f was used to capture three dimensional stereo-images of the implant surface at five areas on each of the 18 randomly selected CPTi surfaces. The average height parameter ( $S_a$ ) of the surfaces studied was measured up to micrometer scale using the IFM 2.1.5 software. For every surface, the area of measurement was within the limit of 40  $\mu\text{m}$  × 40  $\mu\text{m}$  in dimension. Five measurements were taken and an average value and standard deviation of implant surface roughness were calculated henceforth (Nazir *et al.*, 2015).



*Figure 2:* Twin variable grinding and polishing machine (250 High Speed Twin Grinder-Polisher by Buehler) was used for gritting the CPTi surfaces.

### 3.2.2. Sandblasting.

The gritted titanium substrates were then sandblasted to increase their surface roughness by using a sandblasting machine as shown in *Figure 2* (SB-8060-KP Techno Finishing Sdn. Bhd. Malaysia) (Medvedev *et al.*, 2016). Grade A brown alumina of mesh 120 and an average abrasive grain size of  $125\mu\text{m}$  was blasted at a distance of 5cm perpendicular to the sample surface through an air gun for approximately 3 seconds, at a pressure of 50 psi (Nazir *et al.*, 2015). The samples were then rinsed in ethanol and distilled water to remove the sandblasted residua and contaminants from the samples surface, followed by air-blasting until they were dried. The Alicona Infinite Focus Optical 3D Measurement Device G4f was used to measure Average Roughness ( $S_a$ ) of 18 randomly selected samples.



Figure 3: Shows the sandblasting machine (SB-8060-KP Techno Finishing Sdn. Bhd. Malaysia.) used for this study.

### 3.2.3. Acid Etching

The sandblasted CPTi samples were then acid etched by using a mixture of 37% hydrochloric acid (HCl) and 98% sulphuric acid (H<sub>2</sub>SO<sub>4</sub>) with a volumetric ratio of 1:3 respectively. 5mL HCl and 15mL H<sub>2</sub>SO<sub>4</sub> were diluted in 100mL distilled water. This dual acid solution was kept in a water bath of 80°C for 30 minutes and it was ensured that the surface to be etched was facing the acidic solution (Nazir *et al.*, 2015).

The samples were then taken out and cleaned with ethanol and distilled water, followed by air-blasting to dry the titanium surfaces. These acid etched CPTi were observed again under the Alicona Infinite Focus Optical 3D Measurement Device G4f and the average surface roughness (*S<sub>a</sub>*) of 18 randomly selected samples was measured.

#### 3.2.4. Activation of CPTi Surface With The Hydroxyl Group.

After acid etching, the samples were treated with sodium hydroxide (NaOH) so that the surfaces could be activated with hydroxyl groups from the alkaline solution. The CPTi discs were immersed inside a 50mL 5M NaOH solution for 24 hours at 60°C in an oven, followed by rinsing in distilled water and drying at 40°C (Jalota *et al.*, 2006; Nazir *et al.*, 2015).

This NaOH immersion helps in making the inert CPTi surfaces act better against the natural deposition of calcium phosphate in the form of HA. NaOH submersion renders the implant surface to possess a layer of hydrated titanium oxide (HTiO<sub>3</sub>-), which in turn causes hydroxyl groups (TiOH) to appear on the surface, hence enabling the deposition of HA (Barbas, 2016).

### 3.3. Surface Characterization

Following the accomplishment of achieving sandblasted and acid-etched surfaces in this experiment, the aim and objectives of this study required us to coat the CPTi surfaces with HA through a biomimetic method.

#### 3.3.1. HA Coating - Simulated Body Fluid (SBF)

A TRIS-buffered 1.5x Tas-SBF solution was prepared based on the work by Jalota *et al.* (Jalota *et al.*, 2006). The reagents shown in Table 1 were used in particular order and specified quantity for coating the titanium samples with HA/Tricalcium phosphate using a SBF solution. A magnetic stirrer plate (Favorit) was used in order to mix the solution well for 2 hours at a speed of 700 rpm. All the titanium

surfaces were immersed in the Tas-SBF solution and incubated at a temperature of 37°C for a total of 14 days.

In the initial 3 days, the Tas-SBF solution was changed for all samples daily at 24 hour intervals. From the third day onwards, namely, the fifth, seventh, ninth, eleventh and thirteenth day, the Tas-SBF solution was replenished. A total of 14 days of immersion were undertaken in the SBF for all samples.

University of Malaya

Order	Reagent	Weight (g/l)	Purity/Concentration (%)	Batch no.
1	NaCl	9.8184	99.5%	011M01471V
2	NaHCO <sub>3</sub>	3.4023	99.5 –100.5%	SZBC2560V
3	KCl	0.5591	99%	031M02021V
4	Na <sub>2</sub> HPO <sub>4</sub>	0.2129	99%	BCBF0131V
5	MgCl <sub>2</sub> .6H <sub>2</sub> O	0.4574	99%	110M02171V
6	1M HCl	15mL	10 mol	SZBC2490V
7	CaCl <sub>2</sub> .2H <sub>2</sub> O	0.5513	99%	SLBC0871V
8	Na <sub>2</sub> SO <sub>4</sub>	0.1065	99%	051M0064V
9	TRIS*	9.0855	99.8%	BCBK2803V
10	1M HCl	50mL	10 mol	SZBC2490V

*Table 1:* Order and quantity of chemical reagents supplied by Sigma Aldrich Sdn. Bhd mixed to prepare Tas-SBF solution.

### 3.3.2. Surface Analysis Of HA Coated Samples

The Alicona Infinite Focus Optical 3D Measurement Device G4f Metrology was used to evaluate the surface roughness of the SBF immersed samples after the final day of immersion. The Scanning Electron Microscope (SEM) (Low Vacuum Operating Mode, Model number FEI Quanta 250F) was kept at 10 kV, with a Working Distance (WD) of 10mm and varying magnifications to analyze the surface morphology and thickness of the HA layer on top of the CPTi samples. The Fourier Transform Infrared Spectrometer (FTIR Spectrometer) (Model number Nicolet 6700 FTIR, Thermo Scientific.) was used to check the HA/Tricalciumphosphate compound presence and elemental composition of the Tas-SBF coated samples on the 14<sup>th</sup> day.

### 3.3.3. HA Coated Samples Divided Into Randomly Selected Groups.

Three groups were made in this *in vitro* study. Each group consisted of 37 randomly selected discs. The first group, namely the Control Group, had a HA/Tricalcium phosphate compound deposited through the SBF as the surface coating. The second group, the Peptide Group had HA/tricalcium phosphate compound incorporated with RGD on the surface physically adsorbed onto the HA coating. The third group, the Collagen Group had HA/tricalcium phosphate compound and collagen physically adsorbed onto the HA coating as well. In total, a number of 111 samples were prepared for *in vitro* analysis in this study. *Figure 3* shows a simplified flowchart of how the samples were distributed into each of their randomly selected and designated groups.

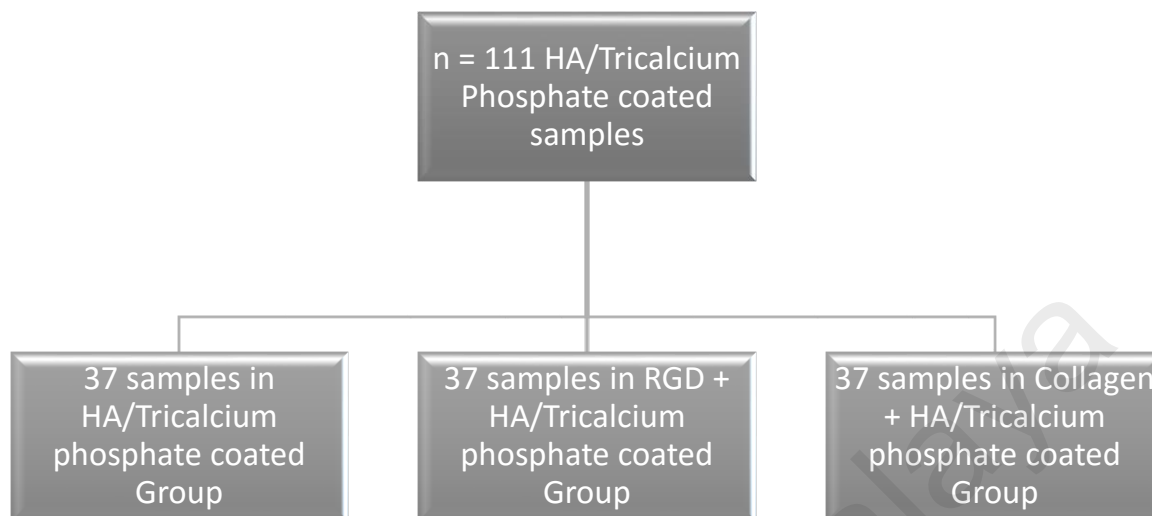


Figure 4: Shows a flowchart of how the samples were divided into three groups.

#### 3.3.4. HA/Tricalciumphosphate Compound Incorporated With RGD

For the Peptide Group, RGD ((Arg-Gly-Asp) (Product Number: A 8052, Molecular Formula:  $C_{12}H_{22}N_6O_6$ ) was obtained from Sigma Aldrich. RGD was handled with care in sterile conditions. RGD is prone to contamination, leading to degradation hence a strict protocol was followed. The RGD was supplied in powder form. Dilution of the powdered RGD was done using sterile water. Eppendorf micropipettes with autoclaved tips were used for dilution and for all procedures. The RGD solution was prepared as mg/ml. Freezing and thawing multiple times may lead to degradation, therefore the RGD solution was aliquoted into 1mg/ml vials and stored at  $-20^{\circ}C$ . The preparation and handling of the peptide was performed according to the manufacturer's instructions.

The HA/tricalcium phosphate coated CPTi substrates were immersed in 0.1M MES buffer solution for 30 minutes.  $20\mu g/ml$  peptide was added to the above buffer solution and the reaction was allowed

to take place for 18 hours at room temperature. After 18 hours, the titanium substrates were carefully removed and rinsed with distilled water so that weak bonded proteins were washed off (Ryuet *et al.*, 2013; C. Yang *et al.*, 2009). To do the surface analysis, the samples were freeze dried at -70°C using a freeze dryer (Model name: FreeZone, Labconco). The temperature of the freeze dryer was set to -50°C and the vacuum pressure was around 0.043mBar. Samples were freeze dried for 6 hours. For surface analysis, the samples were checked under the SEM (Scanning Electron Microscope) and EDS (Energy-dispersive X-ray Spectroscopy) for their morphology and elemental composition respectively.

### 3.3.5. HA/Tricalciumphosphate Compound Incorporated With Collagen.

For the Collagen Group, 0.1% (1 mg/ml) solution of calf skin collagen type I in 0.1 M acetic acid was obtained from Sigma Aldrich (C8919) and was kept at 2-8°C for storage purposes. The collagen solution (1 mg/ml) was diluted 10-fold with sterile water to obtain a working concentration of 0.01%. The diluted solution was stirred for 2hrs at room temperature and the protein was allowed to bind to the CPTi for 18hrs at 2-8 °C. The preparation and handling of collagen was performed according to the manufacturer's instructions. Afterwards, the CPTi substrates were carefully removed and rinsed with distilled water to remove weakly bonded collagen off the surface (Monti, 2007; Nagai *et al.*, 2002). To perform the surface analysis, the samples were freeze dried and checked under the SEM and EDS for their morphology and elemental composition respectively.

### **3.4. In Vitro Cell Study**

The third part of this methodology required the three groups of coated titanium surfaces to be tested *in vitro* for their efficacy at inducing a favorable cell response. In this study, the coated titanium discs were sterilized before culturing primary human osteoblasts onto them. The sterilization was done by autoclaving them at 121°C for 30 minutes at 15psi. All cell culture work was done in the biosafety cabinet (Model: Scanlaf, Mars Safety Class 2).

#### *3.4.1. Coated Titanium Substrates And Their In Vitro Cell Response*

Human Osteoblasts (HOB) from normal human bone (Cryopreserved: 2nd passage, >500,000 cells in Basal Medium containing 10% FBS, 10% DMSO) were acquired from Cell Applications, USA. The cryopreserved vial was stored in a liquid nitrogen storage tank immediately upon arrival. The Transport Medium was removed by aspiration. The HOB were primarily cultured in 25cm<sup>-2</sup> T-flasks and subsequently in 75cm<sup>-2</sup> T-flasks till passage 4 using the Growth Medium (Stock No.: C08-417-500. Cell Applications, USA.) with Dulbecco's Modified Eagle's Medium (DMEM) supplemented with 10% Fetal Bovine Serum(FBS), 1% penstrap (penicillin and streptomycin) at 37°C in a humidified atmosphere with 5% CO<sub>2</sub>. Fresh Growth Medium, 5 ml for a T-25 flask and 15 ml for T-75 flask was added subsequently. The medium was changed every other day. The cells were placed on the coated CPTi discs at a cell density of 1x10<sup>4</sup> cells per disc and cultured for 14 days under the conditions as specified by the manufacturer (Knabe *et al.*, 2002).

For the first two days, the cells were allowed to grow on to the CPTi substrates with Growth Medium. On the proceeding days the Differentiation Medium (Stock Code: C08-417D-250. Cell Applications,

USA.) was added to the cells. The CPTi discs with cells were cultured in 24 well plates. For day 1,3,5,7,9,11, and 14, 3 samples from each group were taken to check for cell viability using the MTT assay. For day 7 and 14, 3 samples from each group were taken to be tested for Alkaline Phosphatase (ALP) activity. For checking the cell morphology, 3 samples from each group were taken on the 7<sup>th</sup> and the 14<sup>th</sup> day. For checking the osteogenesis, 3 samples from each group were stained with Alizarin Red on the 14<sup>th</sup> day of cell culturing.

### *3.4.2. Cell Morphology*

Cell adhesion and spreading was evaluated on day 7 and day 14 of cell culturing. The adherent cells on the discs were rinsed two times with ice cold phosphate buffer saline (PBS) and fixed for 2 hrs in McDowell and Trump's fixative with 4% glutaraldehyde, 1% formaldehyde, and 0.1 M sodium-cacodylated buffer (pH 7.2) and post-fixed in 4% osmium tetroxide for 1 hr. The fixed cell layers were washed with PBS and dehydrated using graded ethanol solutions of 25%, 50%, 75% ,90% and 100% followed by critical point drying which was done using HMDS (Hexamethyldisilazane) solution and allowed to air- dry at room temperature in the fume hood. The samples were then gold coated and the morphology of their surfaces was analyzed using the SEM.

### *3.4.3. Cell Viability And Proliferation*

The 3-[4,5-dimethylthiazol-2-yl]-2,5- diphenyltetrazolium bromide (MTT) assay is a colorimetric assay for assessing cell metabolic activity. NAD(P)H-dependent cellular oxidoreductase enzymes may, under defined conditions, reflect the number of viable cells present. These enzymes are capable

of reducing the tetrazolium dye MTT 3-(4,5-dimethylthiazol-2-yl)-2,5-diphenyltetrazolium bromide to its insoluble formazan, which has a purple colour (Y. Yang *et al.*, 2002).

On days 1, 3, 5, 7, 9, 11, and 14 of cell culturing, the cell viability was analyzed by the MTT assay (B03-30006 MTT Cell Viability Kit, Biotium, USA). Cells which were incubated with 100 $\mu$ L MTT (5 mg/mL) in culture medium at 37°C for 4 hrs (Mariscal-Muñoz *et al.*, 2016). The medium was then aspirated from the well, and 1 mL DMSO (dimethyl sulphoxide) was added to each well. The plates were then stirred on a plate shaker for 5 min. The optical density was read at 570 nm on a plate reader (Model: Infinite M200 Pro, Tecan), and the data was expressed as absorbance.

#### 3.4.4. Cell Differentiation

Alkaline Phosphatase (ALP) catalyzes the hydrolysis of phosphate esters in alkaline buffer and produces an organic radical and inorganic phosphate. The change in alkaline phosphatase level and activity is associated with a lot of diseases in the liver and bones. Alkaline phosphatase is also a popular enzyme conjugated to secondary antibody in ELISA. In Alkaline Phosphatase Fluorometric Assay Kit (D01-K422-500 ALP Fluorometric Kit, Biovision, USA.), ALP cleaves the phosphate group of the non-fluorescent 4-Methylumbelliferyl phosphate disodium salt (MUP) substrate resulting in an intense fluorescent signal (Lincks *et al.*, 1998).

In this study, ALP activity was assayed at day 7 and 14 of cell culturing using the ALP fluorometric assay kit (Mariscal-Muñoz *et al.*, 2016). In accordance with the distributor's protocol, inhibitors of ALP, like tartrate, fluoride, EDTA, oxalate, and citrate, were avoided in sample preparation. The cell culture media was assayed directly and centrifuged to remove insoluble material at 13,000g for 3

minutes. The test samples were added directly into 96-well plates, and the total volume was brought to 110µl with Assay Buffer. In order to avoid interference of components in the sample, a sample background control was set also. The same amount of samples were added into separate wells, and the volume was brought to 110µl. This was mixed well and incubated for 30min at 25°C, in the dark. Then all reactions were stopped by adding 20µl of stop solution except the background control. The plate was read at 440nm in a microplate reader (Model: Infinite M200 Pro, Tecan).

#### 3.4.5. Alizarin Red S. Staining - Detection of Calcium Deposits (Mineralization)

Osteoblasts can induce mineralization and produce extracellular calcium deposits *in vitro*. Calcium deposits are an indication of successful *in vitro* bone formation and can specifically be stained bright orange-red using Alizarin Red S. staining method (Jeong & Jeong, 2016).

In this study, after 14 days of incubation, two samples from each group were assessed for mineralization. The cells were washed with PBS after aspiration of the medium. Formalin (10%) was added to the wells to cover the cellular monolayer for 30 minutes. This was done to fixate the cells. Then the samples were subjected to Alizarin Red S. staining solution (R03-9872-10 Alizarin Red S, 1% Indicating Solution, R&M, UK) to cover samples. This was then incubated at room temperature in the dark for 45 minutes. The samples were washed with 1ml distilled water four times and PBS was added to the wells. The surfaces were then analyzed under a compound microscope (High Resolution Compound Microscope, Model: Olympus). Undifferentiated HOB, without extracellular calcium deposits, is slightly reddish, whereas mineralized osteoblasts, with extracellular calcium deposits appear bright orange-red.

### 3.4.6. Statistical Analysis

The Statistical Package for the Social Sciences (SPSS v.22.0, IBM, Armonk, NY, USA) was used for the analysis (B.-A. Lee *et al.*, 2014). Statistical significance was defined as  $P < .05$ . The surface roughness measurements at each stage of the surface modifications and HA coatings were analyzed via one-way analysis of the variance (ANOVA). The MTT Assay absorbance readings were evaluated using ANOVA as well. The ALP Assay absorbance readings were descriptively assessed by the same software.

University of Malaya

## CHAPTER 4 – RESULTS

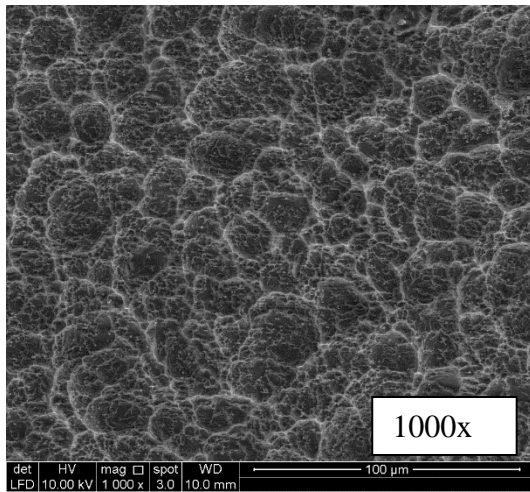
The results of this study will be presented by showing the morphology and the average roughness changes and results of the samples in the initial phases of the experiment. Subsequently, surface characterization and finally the *in vitro* results will be highlighted.

### 4.1. Surface Modifications

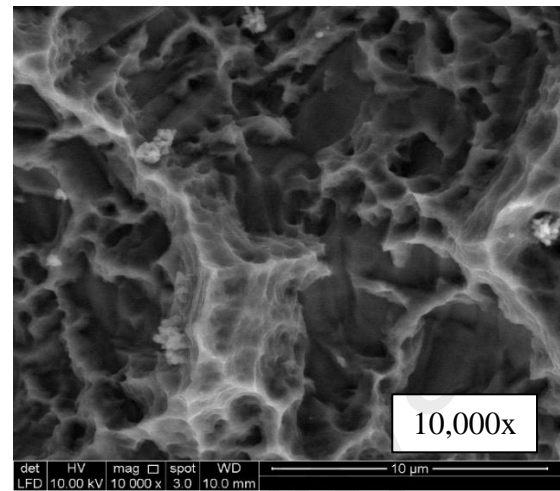
The first part of the experiment constituted of surface modifications of the CPTi samples. This comprised of subjecting the samples to firstly gritting, secondly sandblasting, and thirdly acid-etching.

#### 4.1.1. SEM Analysis Of Acid Etched Surfaces

When the SEM was used to analyze pre-HA/Tricalcium phosphate coated samples, the acid etched surfaces showed multiple pits and craters. CPTi samples contained a uniform and well-defined porous surface. In addition to small acid induced indentations, the surfaces displayed large concavities that were induced by the sandblasting process that preceded acid etching. *Figure 5A* and *5B* show the SEM micrographs of the acid etched surfaces of CPTi.



5A



5B

*Figure 5A & 5B:* Show the SEM image of Acid-Etched samples at 1000x and 10,000x magnification with a voltage of 10 kV and a Working Distance (WD) of 10mm.

#### 4.1.2. Average Roughness Results Of Surface Modifications

Descriptive analysis of the surface roughness profiles of the samples, using  $S_a$  values, showed that for sandblasted and acid etched samples CPTi displayed a higher  $S_a$  than a gritted or polished CPTi surface. The most disordered values for  $S_a$  were obtained in the sandblasting phase of the experiment. The sandblasted samples showed an average  $S_a$  value of  $2.48 \pm 0.74 \mu\text{m}$ . The acid-etched samples displayed a lesser roughness than their sandblasted and gritted counterparts, that is, an average  $S_a$  of  $2.35 \pm 0.18 \mu\text{m}$ . Within the HA/Tricalcium phosphate coated samples, there was a general increase in  $S_a$  in all surfaces involved. The HA/Tricalcium phosphate coatings on the 14<sup>th</sup> day showed average  $S_a$  values of  $2.74 \pm 0.28 \mu\text{m}$ . Graphical representations of this data is shown in *Figure 6* and *Figure 7*.

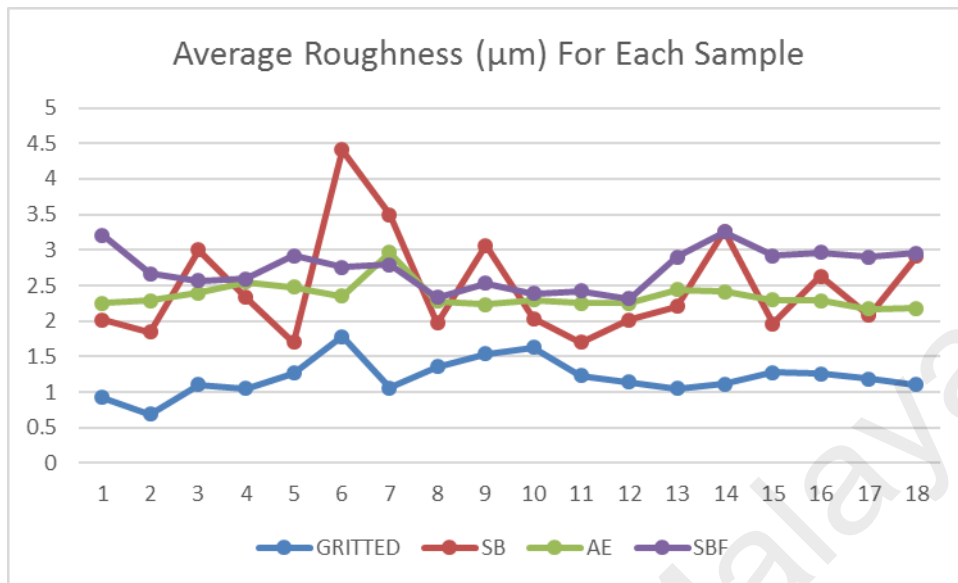


Figure 6: Shows a graphical representation of the average  $Sa$  values obtained for each sample.

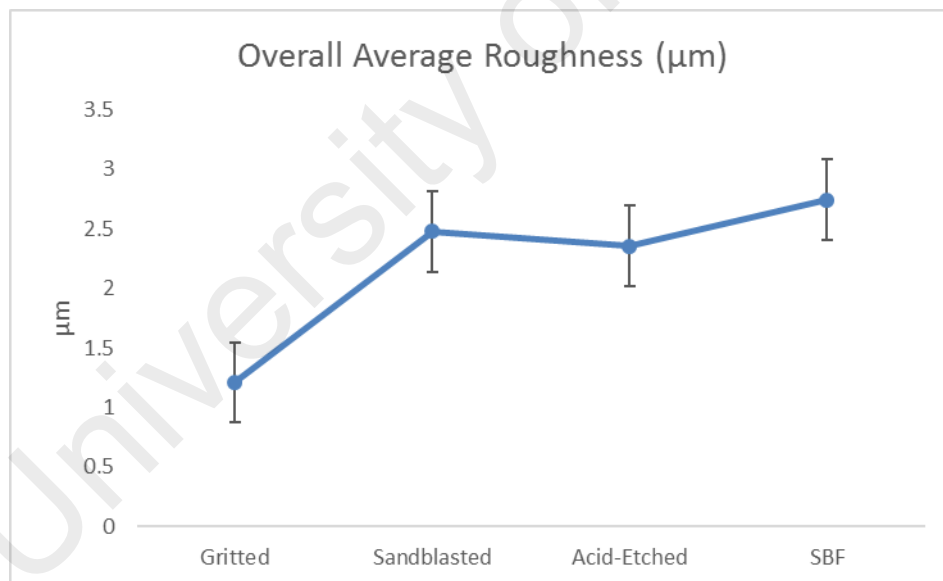


Figure 7: Shows a graphical representation of the overall  $Sa$  values obtained for all the samples.

$Sa$  value of the samples were obtained and the results of the first phase of the experiment were evaluated using SPSS. When ANOVA was conducted for the attained data, it showed that there was a significant difference amongst the various groups ( $P < 0.001$ ) This can be seen in *Table 2*. The gritted samples showed an average  $Sa$  of  $1.21 \pm 0.25\mu\text{m}$  which was significantly lower than all the

other groups ( $p < 0.001$ ). The Tas-SBF group produced the highest roughness that was significant compared to Acid Etched samples ( $P < 0.001$ ) but not significant compared to Sandblasted samples ( $P = 0.55$ ). There was no significant difference seen between Acid Etched samples and Sandblasted samples.

Groups	Df	F	P value
Gritted SB AE Tas-SBF	3	65.524	<.0001

Table 2: Shows significant difference amongst the various groups.

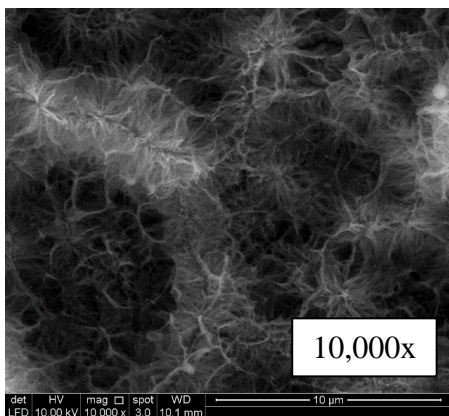
## 4.2 Surface Characterization

After achieving a desirable roughened CPTi discs, the samples were coated with HA, RGD and collagen and the surfaces were analysed. This section of the results explains the data that was obtained.

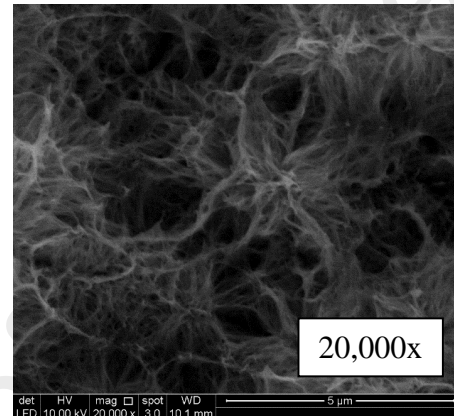
### 4.2.1. Biomimetic HA Coating Morphology

Proceeding the gritting, sandblasting, acid etching and Tas-SBF immersion processes were sequentially to modify the surfaces of the CPTi substrates, the 14 day old Tas-SBF immersed samples needed to be analyzed for the morphology of their HA/Tricalcium phosphate coatings under the SEM. The Tas-SBF HA/Tricalcium phosphate coated surfaces possessed a crystalline coating indicated by an intricate crystal assembly that resembled a “flower-like” structure. This is typical of the formation

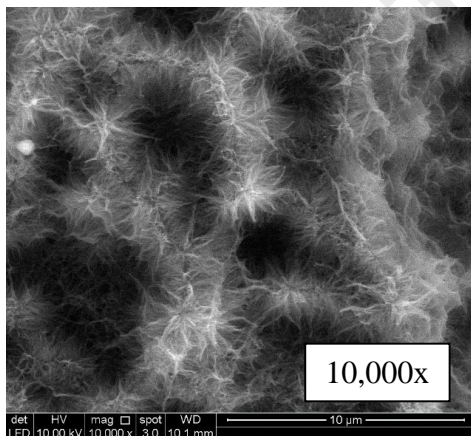
of HA and calcium phosphate crystals that deposit from the Tas-SBF solution. The crystal size of the coating was greater on the 14<sup>th</sup> day of immersion into Tas-SBF as compared 7<sup>th</sup> day. The flower like HA/Tricalcium phosphate structures also show a denser and better woven texture on the 14<sup>th</sup> day of Tas-SBF immersion. Fig. 11A, 11B, 11C, and 11D show the SEM micrographs of the HA coating on 7<sup>th</sup> and 14<sup>th</sup> day at 10,000x and 20,000x magnification respectively.



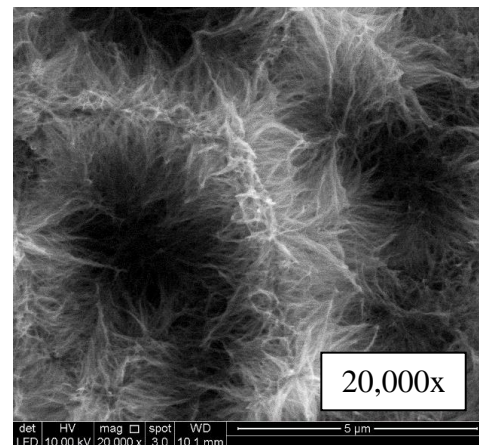
8A



8B



8C

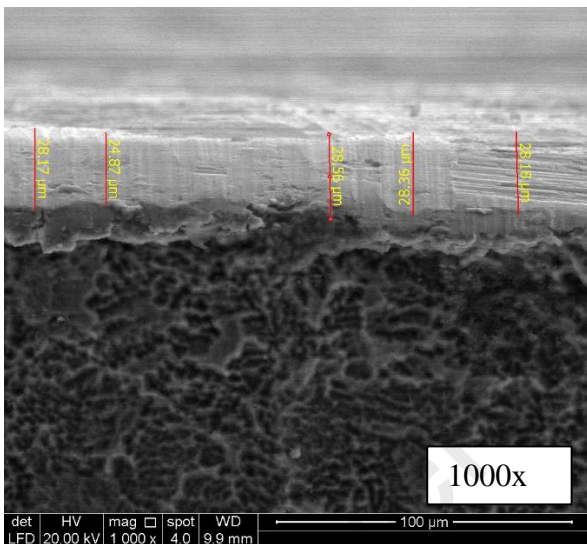


8D

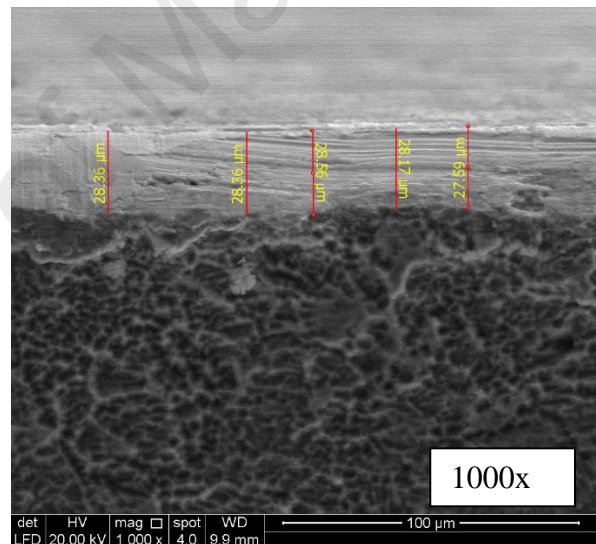
*Figures 8A & 8B:* Show 7<sup>th</sup> day samples. *Figures 8C & 8D:* Show 14<sup>th</sup> day samples under the SEM containing HA/Tricalcium phosphate coating at 10,000x and 20,000x magnification respectively. The samples were subjected to a voltage of 10 kV and a Working Distance (WD) of 10mm under the Scanning Electron Microscope (SEM).

#### 4.2.2. HA Coating Thickness

With the help of the SEM, at a voltage of 10 kV, a Working Distance (WD) of 10mm, and a magnification of 1000x, the thickness of the coated surfaces was also measured for the samples on the 14<sup>th</sup> day of immersion in the Tas-SBF solution. *Figures 9A and 9B* show the thickness of the surface coating on the 14<sup>th</sup> day of Tas-SBF immersion. The average thickness of the HA/Tricalcium phosphate was  $28.26 \pm 0.28\mu\text{m}$ .



9A



9B

*Figures 9A and 9B:* Show the thickness of the samples on the 14<sup>th</sup> day of Tas-SBF immersion.

#### 4.2.3. The FTIR Results

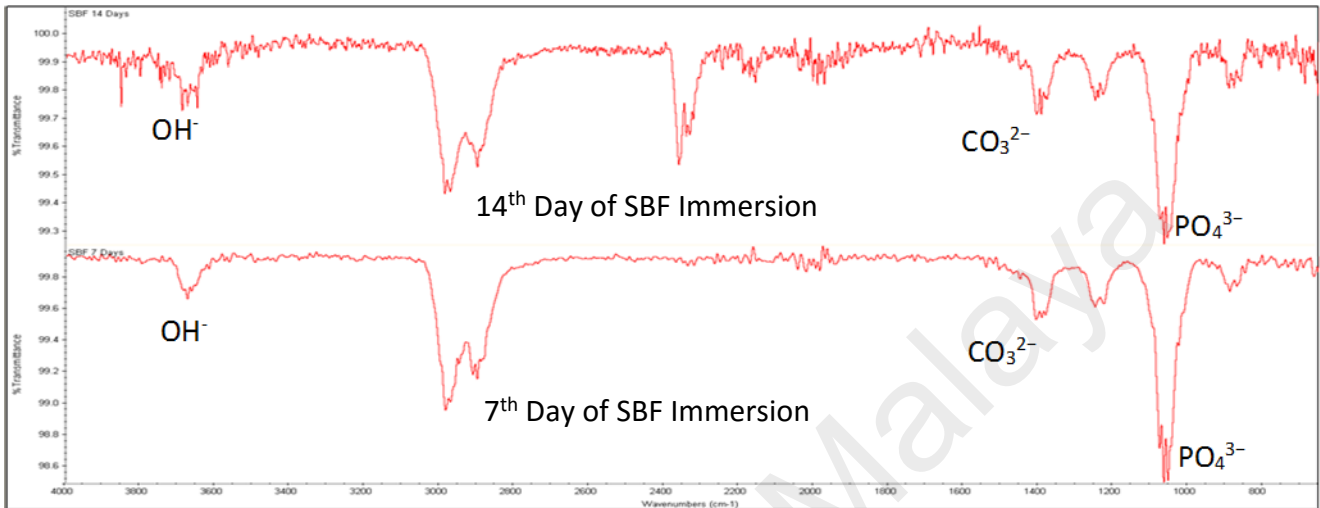


Figure 10: Shows the FTIR of the surface coatings after 14 days of TAS-SBF immersion.

The FTIR was used to obtain an infrared spectrum of transmittance of HA/Tricalcium Phosphate on the surface of the samples. This technique was used to ascertain the presence of HA/tricalcium phosphate on the CPTi surfaces after Tas-SBF immersion for 14 days. The absorption bands at 1400–1550 $\text{cm}^{-1}$  are the peak of  $\text{CO}_3^{2-}$  group and 560–600 $\text{cm}^{-1}$  and 1030–1090 $\text{cm}^{-1}$  are the characteristic peaks of the  $\text{PO}_4^{3-}$  group, whereas bands around 3500 $\text{cm}^{-1}$  show the presence of  $\text{OH}^-$  groups (Whitehead, Lacefield, & Lucas, 1993). Figure 10 shows the FTIR spectrum peaks for day 7 and day 14 of Tas-SBF immersion. Analysis with the FTIR spectrum for the Tas-SBF coatings on the 7<sup>th</sup> and the 14<sup>th</sup> days of immersion of CPTi surfaces showed a gradual elevation in the peak intensity linked with an increase in the number of Tas-SBF immersion days. With the results of the FTIR spectrum alone it was not possible to deduce that HA/Tricalcium phosphate was present on the sample surfaces. Hence, additional analytical evaluation was required. The EDS was employed to fulfil this analytical query.

4.2.4. EDS results of HA/Tricalcium phosphate Coated Samples

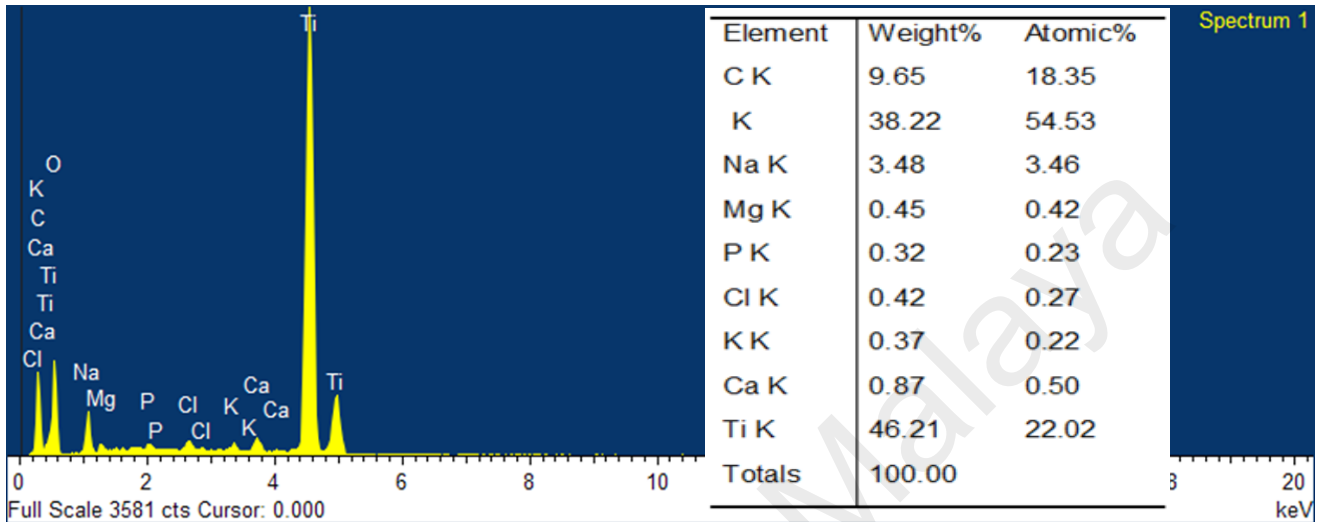


Figure 11A

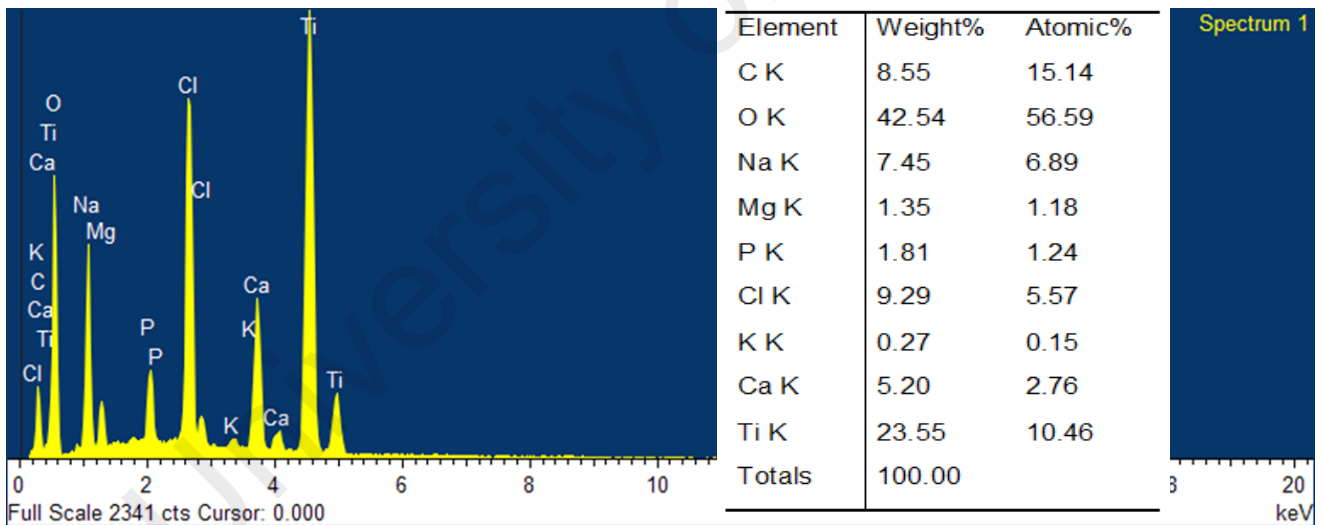


Figure 11B

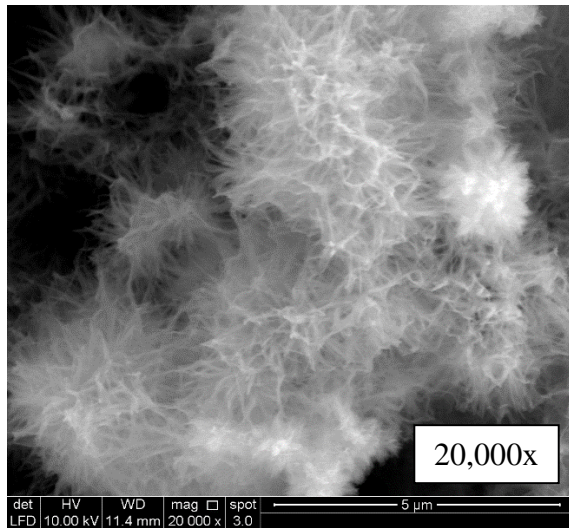
Figures 11A & 11B: Show the EDS elemental analysis of CPTi surfaces coated with HA/Tricalcium phosphate on the 7<sup>th</sup> and 14<sup>th</sup> day.

The EDS analytical technique was used for elemental analysis HA/Tricalcium phosphate surface coating of the CPTi substrates on the 7<sup>th</sup> and 14<sup>th</sup> day of Tas-SBF immersion. The EDS results showed

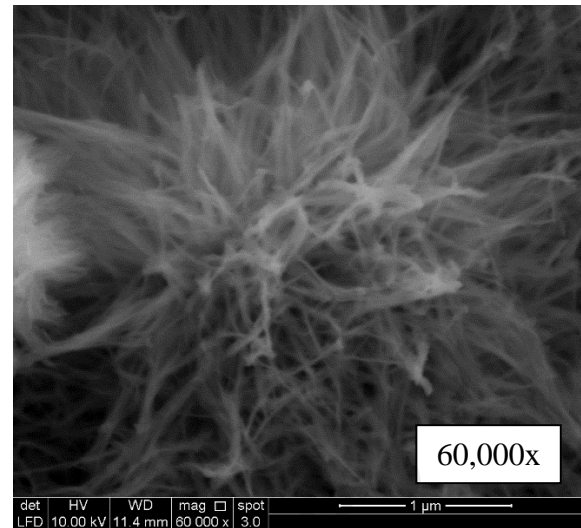
that CPTi produced its typical Ti peaks on both the 7<sup>th</sup> and the 14<sup>th</sup> samples. For the 7<sup>th</sup> day of immersion in Tas-SBF, it can be seen in *Figure 11A* that Ca, P, and O from the HA/tricalcium phosphate are present on the surface. *Figure 11B* shows a higher concentration of Ca, P, and O resulting from the formation of HA/Tricalcium phosphate from the Tas-SBF solution. The average Ca/P ratio of the coating on the 7<sup>th</sup> day of Tas-SBF immersion was approximately 2:1 and for the 14<sup>th</sup> day, it was 3:1. There were no impurities detected from the sandblasting process or the coating methodology ensuring success of the HA/tricalcium phosphate coating. A tabulated form of the elemental analysis that was obtained from the EDS is also shown *Figures 11A & 11B* to further confirm the ratio and the presence of HA/Tricalcium phosphate on the surface of the Tas-SBF immersed samples.

#### 4.2.5. RGD Incorporated HA Coating Morphology

After the process of modifying the surfaces and adding HA onto them was accomplished. For the RGD group, the incorporation of RGD onto the HA/Tricalcium phosphate layer through physical adsorption produced surfaces with flower like RGD deposition. The RGD seemed to be well intertwined with the morphology of the HA crystals. The underlying HA was visible when the surfaces were morphologically assessed. *Figures 12A and 12B* show the SEM micrographs of the composite layer of RGD with HA/Tricalcium phosphate.



12A



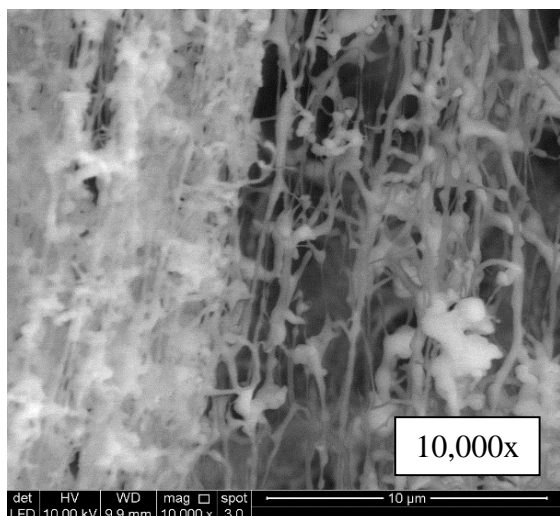
12B

*Figures 12A and 12B:* Show freeze dried Peptide Group samples at a magnification of 20,000x & 60,000x at a voltage of 10 kV and a Working Distance (WD) of 10mm under the SEM.

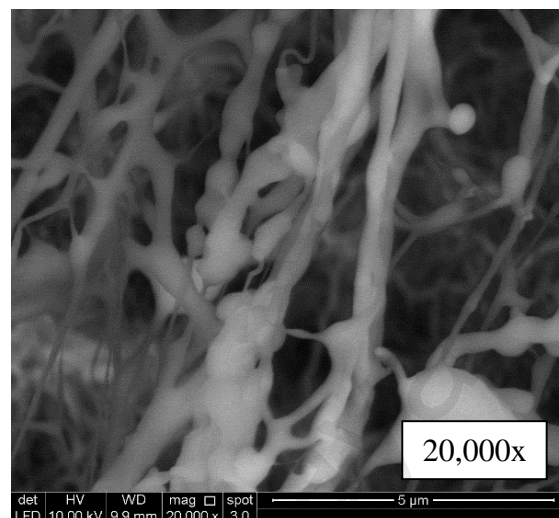
#### 4.2.6. Collagen Incorporated HA Coating Morphology

In the next step of surface characterization, collagen was added onto the HA/Tricalcium phosphate layer through physical adsorption. Collagen was bound to the HA/Tricalcium phosphate coating and showed a scaffold on the surface with strands extending and connecting with each other. The surfaces seemed to be completely covered with collagen strands and the base HA material was nearly invisible.

*Figures 13A and 13B* show the SEM images of the composite layer of collagen with HA/Tricalcium phosphate.



13A



13B

*Figures 13A and 13B:* Show freeze dried Collagen Group samples at a magnification of 10,000x & 20,000x at a voltage of 10 kV and a Working Distance (WD) of 10mm under the SEM.

University of Malak

4.2.7. EDS of RGD and Collagen Groups

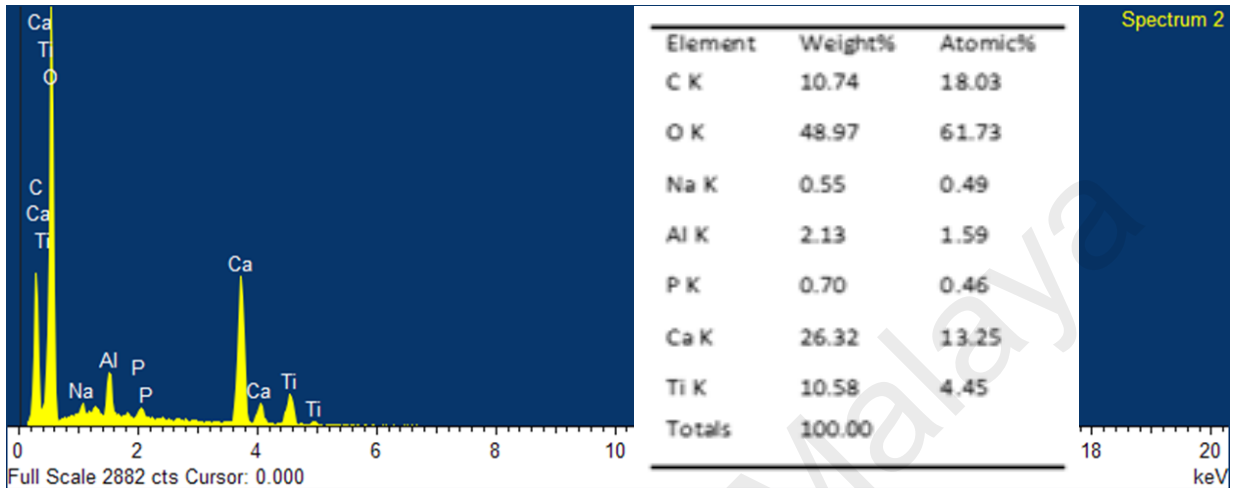


Figure 14A

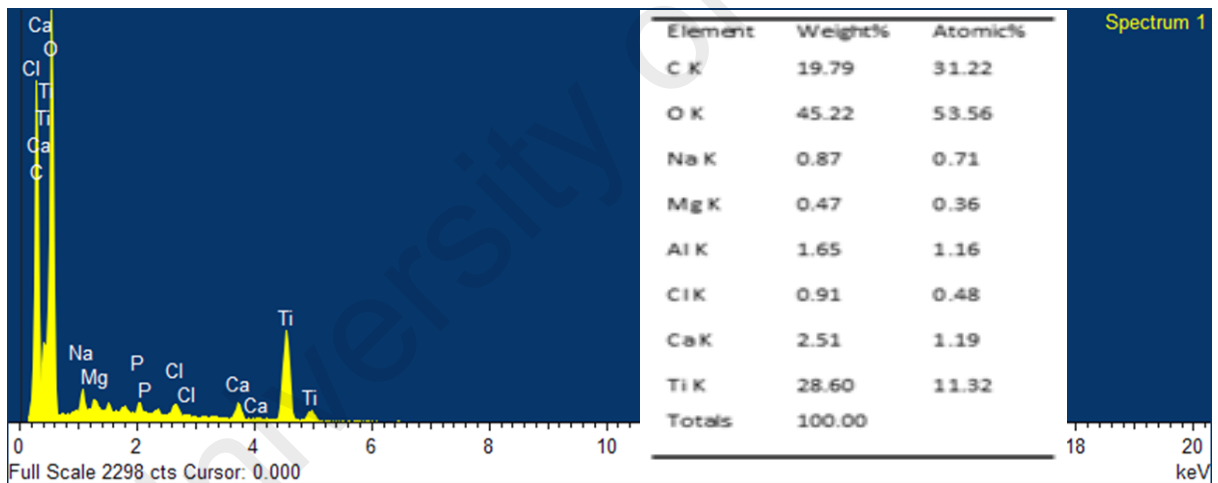


Figure 14B

Figures 14A & 14B: Show the EDS elemental analysis of the RGD Group and the Collagen Group respectively.

After viewing freeze dried samples under the SEM, a confirmatory EDS analytical technique was used for the chemical characterization of RGD with HA/Tricalcium phosphate and Collagen with HA/Tricalcium phosphate surface coatings. The EDS results showed that CPTi produced its

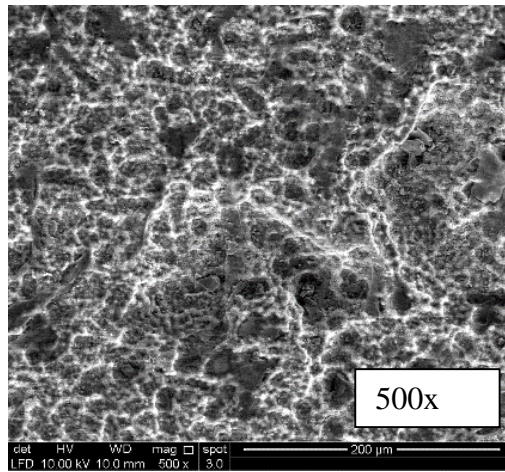
typical substrate Ti peaks on both the samples. For the RGD Group the carbon (C) content showed lesser of a peak than in the Collagen Group. *Figures 14A & 14B* also show peaks of Ca, P, and O resulting from the underlying coating of HA/Tricalcium phosphate. The average C content was  $10.69 \pm 0.22\%$  in weight percentage for the RGD Group. For the Collagen Group the C content was  $19.50 \pm 0.39\%$  in weight percentage. Tabulated elemental analysis of the samples can also be seen *Figures 14A & 14B*.

### **4.3 The *In Vitro* Results**

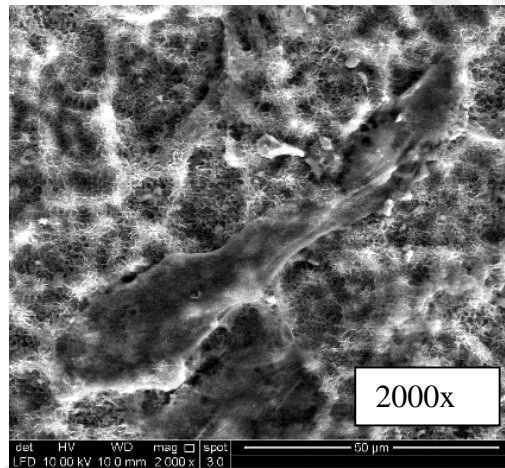
After performing the surface modifications and the surface characterizations, the three groups were tested for osteoblastic cell response in vitro so that their efficacy as osseointegrative and osteoconductive implantable surface materials could be evaluated.

#### *4.3.1. Cell Morphology - SEM Analysis*

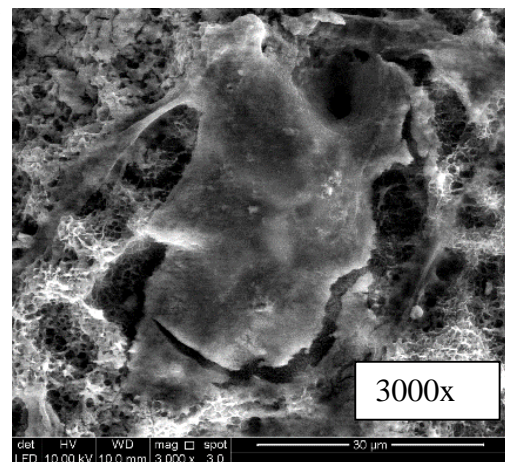
The morphology of the cells on the surface was seen through the SEM. It can be seen from *Figures 15 A-C* that on the 7<sup>th</sup> day of cell culturing, the HA/Tricalcium Phosphate Group and the Peptide Group, *Figures 15 D-F*, showed lesser cellular response than the Collagen Group, *Figures 15 G-I*. The Collagen Group showed the best morphology of the cells followed by the Peptide Group and the HA/Tricalcium Phosphate Group on the 7<sup>th</sup> day.



15A

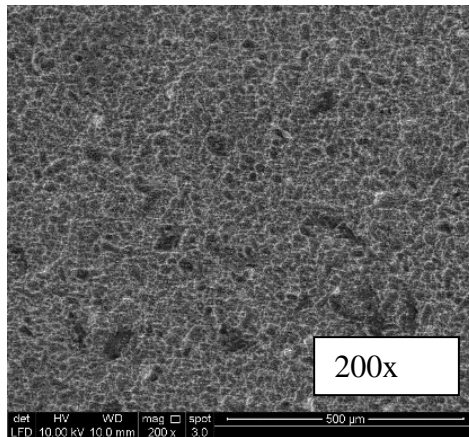


15B

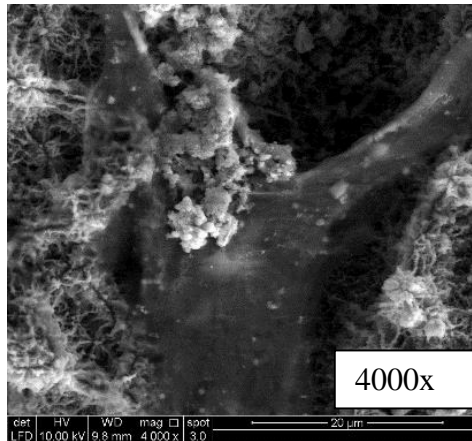


15C

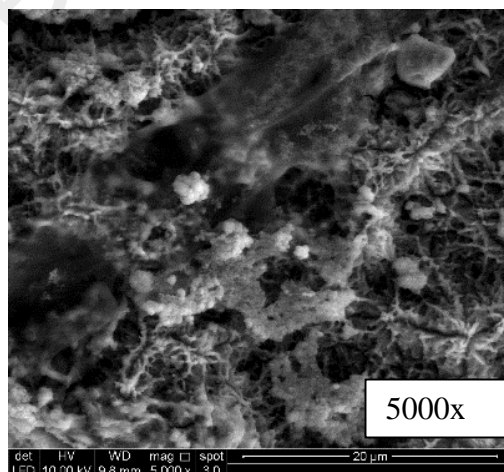
Figures 15 A-C: Show the cell morphology of the HA Group on the 7<sup>th</sup> Day.



15D

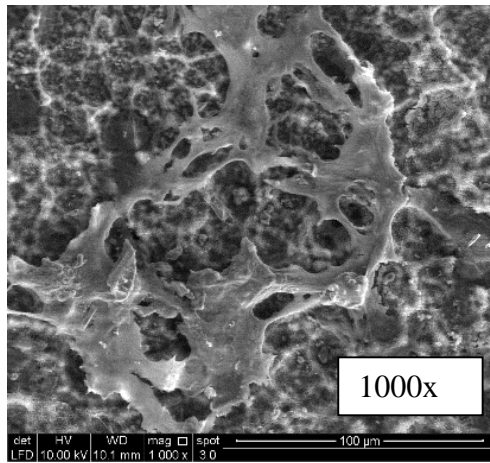


15E

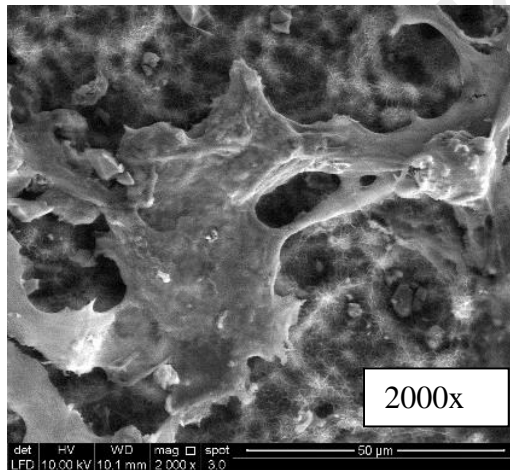


15F

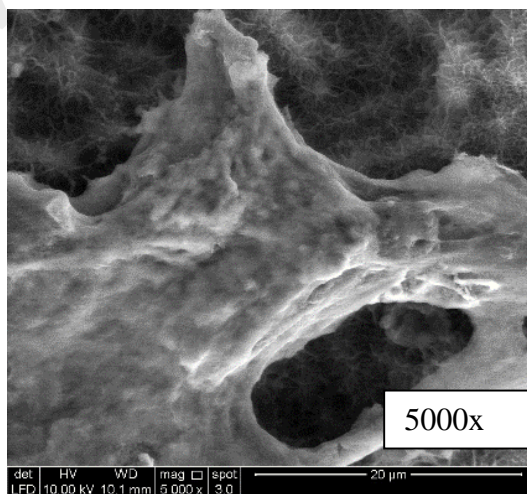
Figures 15 D-F: Show the cell morphology of the Peptide Group on the 7<sup>th</sup> Day.



15G



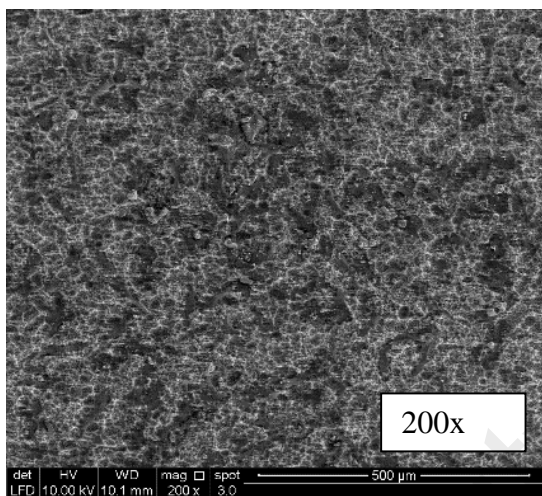
15H



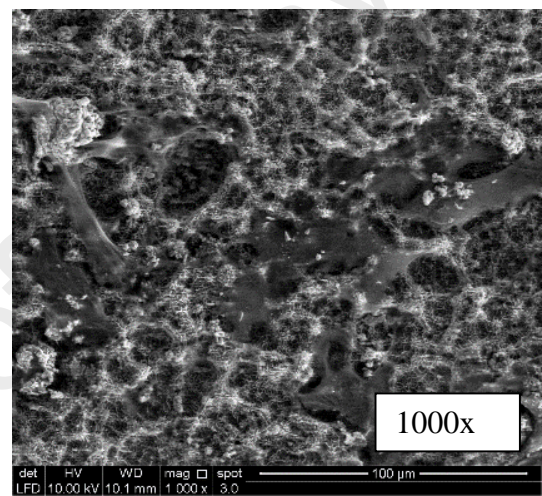
15I

Figures 15 G-I: Show the cell morphology of the Collagen Group on the 7<sup>th</sup> Day.

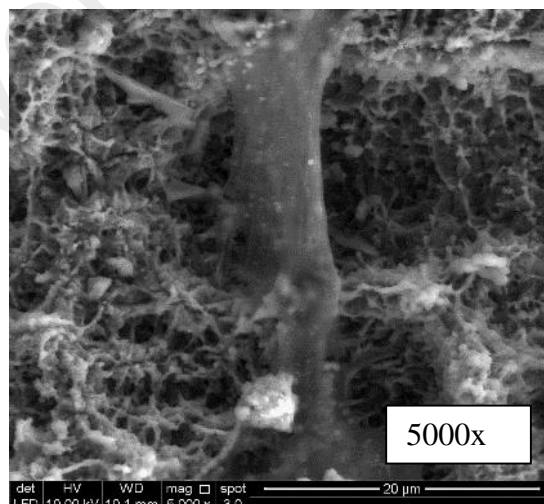
On the 14<sup>th</sup> day of cell culturing, It can be seen from *Figures 16 A-C* the HA Group and the Peptide Group, *Figures 16 D-F*, still showed lesser cellular activity than the Collagen Group, *Figures 16 G-I*. The Collagen Group showed the best morphology of the cells followed by the HA Group and Peptide Group on the 14<sup>th</sup> day of cell culturing respectively.



16A

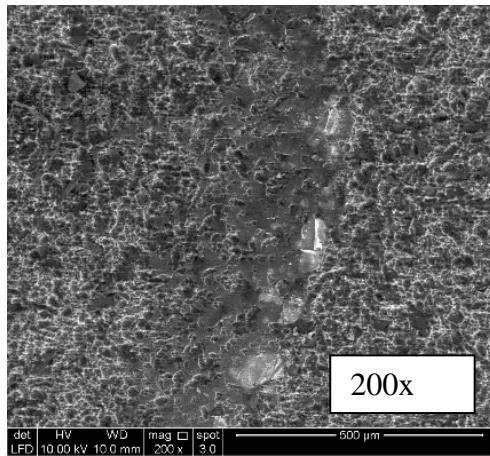


16B

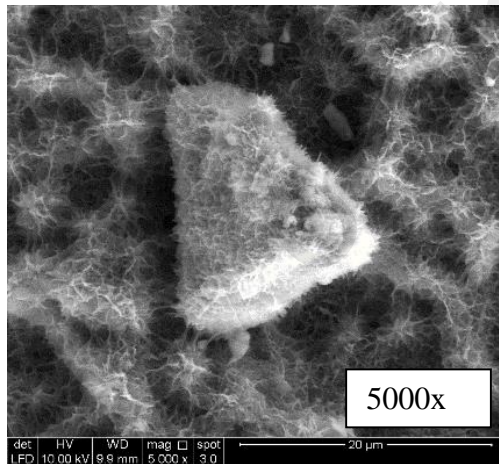


16C

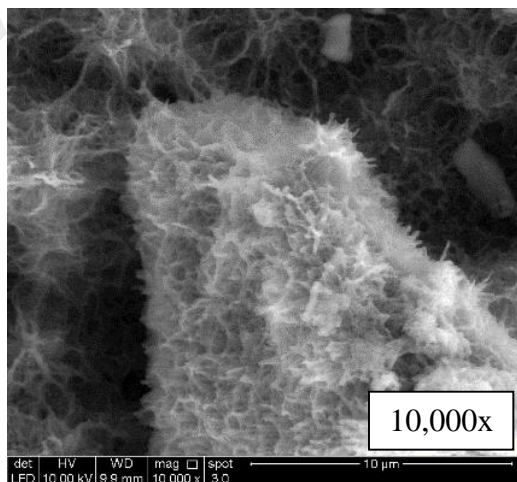
*Figures 16 A-C*: Show the cell morphology of the HA Group on the 14<sup>th</sup> Day.



16D

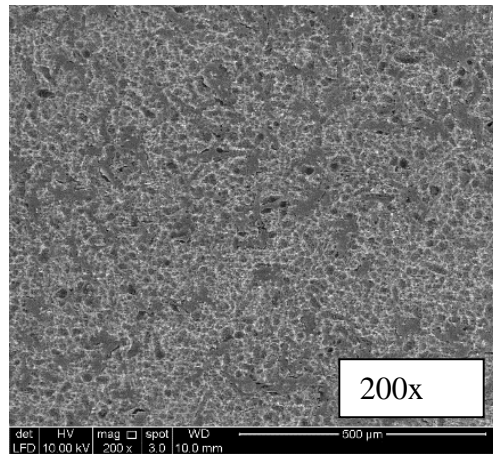


16E

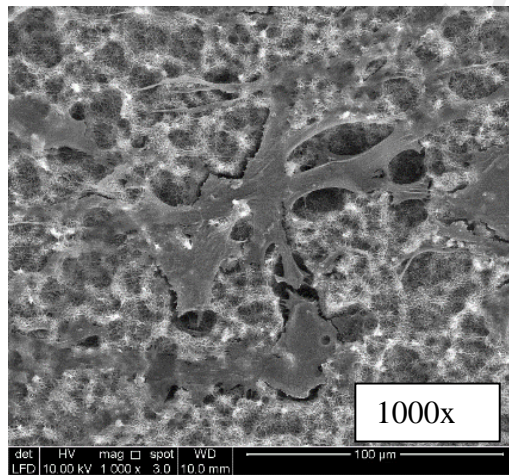


16F

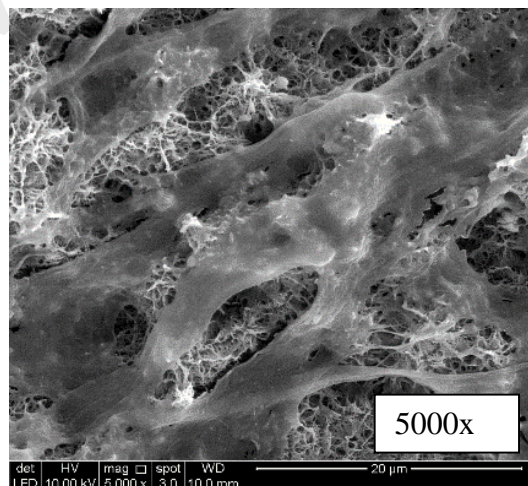
Figures 16 D-F: Show the cell morphology of the Peptide Group on the 14<sup>th</sup> Day.



16G



16H



16I

Figures 16 G-I: Show the cell morphology of the Collagen Group on the 14<sup>th</sup> Day.

#### 4.3.2. MTT Assay – Cell Viability Results

At days 1, 3, 5, 7, 9, 11, and 14 of cell culturing, cell viability was evaluated by the MTT Assay. A graphical representation of the descriptive analysis for the three groups on each day of the MTT Assay is shown in *Figure 15*. The HA group showed a drop in cell viability on Day 5 and it did not fully recover from its downfall since that time. It was seen that on Day 7 the cell viability was the least for the HA group. When Day 7 and Day 14 results were compared within the HA group, the cell viability showed no significant difference. For the RGD group, the cell viability peaked at Day 7 and then dropped drastically by Day 9 to nearly plateau off at the end on Day 14. The Collagen group showed the most stable results where the cell viability gradually increased and showed significant results with respect to time.

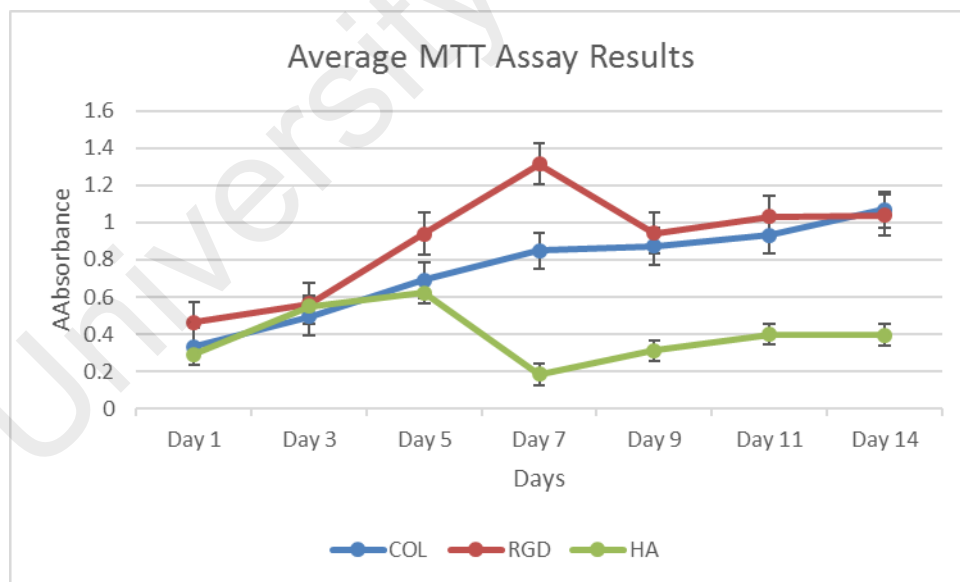


*Figure 17:* Shows the descriptive average MTT Assay results graphically.

To further analyze the cell viability results, a parametric ANOVA test was employed to evaluate the variance between the types of coatings on each day. The results showed that there was no significant

difference amongst the coatings in terms of cell viability on days 1, 3 and 7 ( $P > 0.05$ ). However, there was a significant difference in cell viability between types of coatings on days 7 ( $P = 0.03$ ), 9, 11 and 14 ( $p < 0.001$ ) as shown in the *Table 3*.

Days		Sum of Squares	df	Mean Square	F	Sig.
MTT Day 1	Between Groups	.048	2	.024	.610	.574
	Within Groups	.235	6	.039		
	Total	.282	8			
MTT Day 3	Between Groups	.008	2	.004	.070	.933
	Within Groups	.357	6	.060		
	Total	.365	8			
MTT Day 5	Between Groups	.167	2	.084	1.107	.390
	Within Groups	.454	6	.076		
	Total	.621	8			
MTT Day 7	Between Groups	1.929	2	.965	16.820	<b>.003</b>
	Within Groups	.344	6	.057		
	Total	2.273	8			
MTT Day 9	Between Groups	.717	2	.358	104.216	<b>.000</b>
	Within Groups	.021	6	.003		
	Total	.737	8			
MTT Day 11	Between Groups	.696	2	.348	156.596	<b>.000</b>
	Within Groups	.013	6	.002		
	Total	.709	8			
MTT Day 14	Between Groups	.863	2	.431	89.945	<b>.000</b>
	Within Groups	.029	6	.005		
	Total	.892	8			

*Table 3:* Shows the parametric ANOVA test to analyze the variance between the types of coatings on each day of the MTT Assay analysis.

The Bonferroni pairwise comparison was also performed to detect the difference among groups for days 7 and 9. Due to the non-homogeneity of variance in day 11 and 14, Dunnett T3 pairwise comparison was done to detect the difference among groups for these days. The results showed that the HA group was significantly different from both RGD and Collagen ( $P < 0.05$ ) with no significant difference between RGD and Collagen ( $p > 0.05$ ) (Refer to Appendix D).

To evaluate the overall effect of time on cell viability for each coating used, a series of parametric ANOVA test were conducted for each group again. The results showed the mean of cell viability was significantly affected by time for the Collagen Group ( $p < 0.001$ ) and the Peptide Group ( $P = 0.002$ ) but not for the HA control group ( $P > 0.05$ ) as shown in *Table 4*.

		<b>Sum of Squares</b>	<b>df</b>	<b>F</b>	<b>Sig.</b>
CoatingCOL	Between Groups	1.203	6	22.706	.000
CoatingRGD	Between Groups	1.540	6	6.599	.002
CoatingHA	Between Groups	.413	6	1.230	.349

*Table 4:* Shows the parametric ANOVA results for each of the three groups for the MTT Assay.

#### 4.3.3. ALP Assay Results

After assessing the viability of the cells, it was important to evaluate cell proliferation of the osteoblasts. ALP activity was assessed on the 7<sup>th</sup> and the 14<sup>th</sup> day of cell culturing. The readings from the microplate reader are shown in *Table 5*. For both, the 7<sup>th</sup> and the 14<sup>th</sup> day, ALP Assay showed higher readings as time progressed indicating that there was an increase in cell proliferation. *Figure 16* shows a graphical representation of the average values of the ALP Assay results. It can be seen that on the 7<sup>th</sup> day, the ALP activity was similar for all three group but there was a significant increase of ALP activity in the Collagen group on the 14<sup>th</sup> day when the other groups were compared with it. Between the Peptide and the HA groups there was almost a similar response when ALP Assay was performed.

	<b>Collagen</b>	<b>RGD</b>	<b>HA</b>
Day 7	0.15125	0.1494	0.1761
Day 14	0.30255	0.2026	0.19755

*Tables 5:* Shows the results of the ALP Assay on days 7 and 14 respectively.

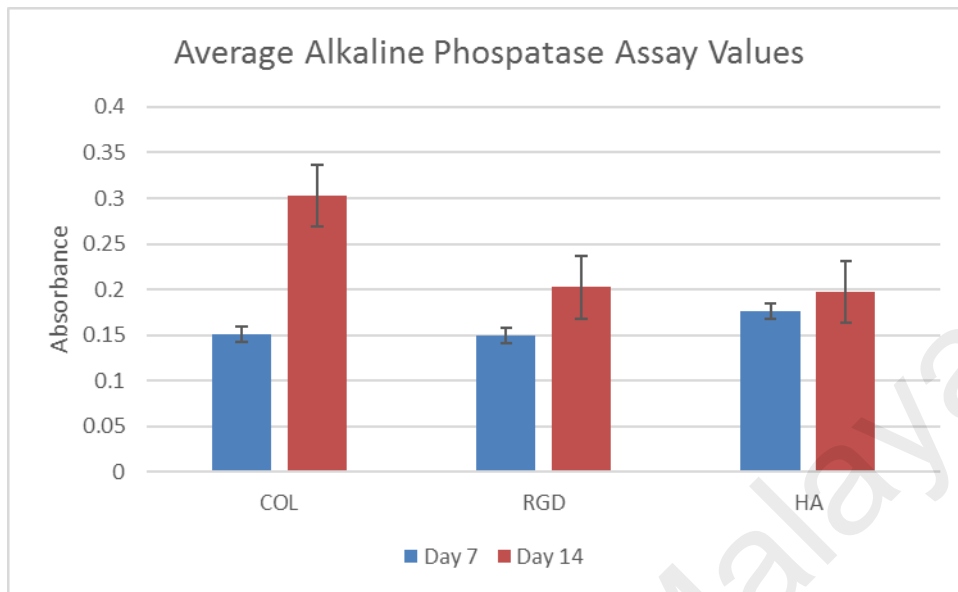
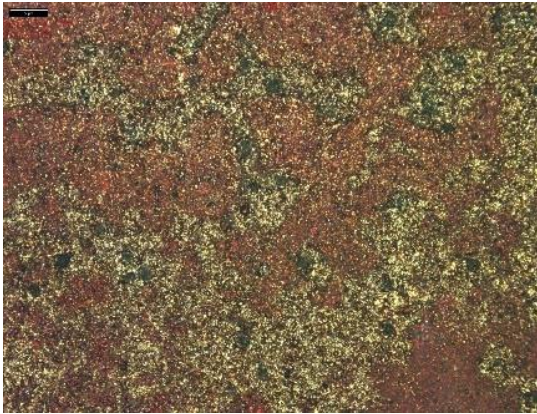


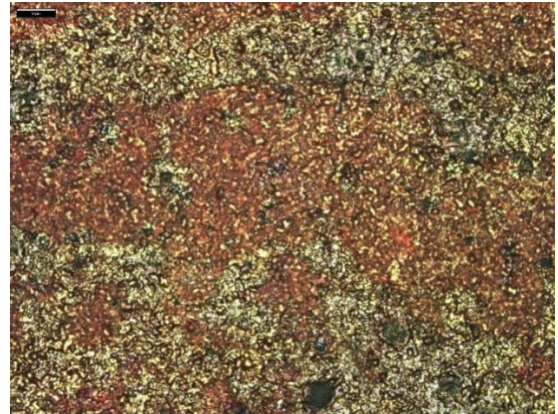
Figure 18: Shows a bar chart of the average values of the ALP Assay.

#### 4.3.4. Alizarin Red Staining - Detection of Calcium Deposits (Mineralization)

After evaluating the morphology, cell viability and cell proliferation of the surfaces in this study, the osteoblasts on the samples in the three groups were analyzed for the occurrence of mineralization Alizarin Red S. staining method. Figures 19A shows the resulting image of the HA Group under a compound microscope of the mineralization achieved after 14 days of cell culturing. Figures 19B shows the mineralization for the Peptide Group and Figures 19C shows the same for the Collagen Group. The greatest mineralization achieved among the three groups was on the Collagen Group followed by the Peptide Group and then the HA/Tricalcium phosphate Group.

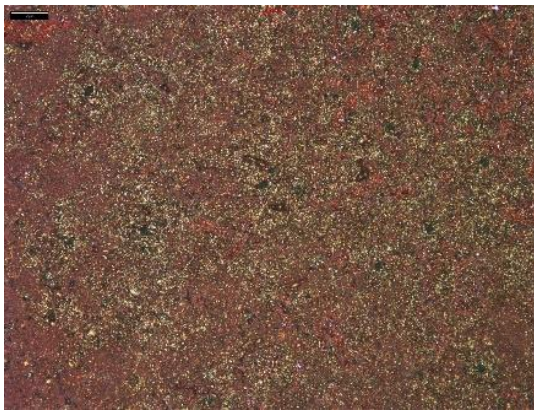


19A



19B

Figures 19 A-B: Show the mineralization on the HA Group samples.



19C



19D

Figures 19 C-D: Show the mineralization on the Peptide Group.



19E



19F

Figures 19 E-F: Show the mineralization on the Collagen Group.

## CHAPTER 5 – DISCUSSION

### 5.1 Surface Modifications

The speed of healing in implant therapy after implant insertion and the quality of the bone-implant interface henceforth has been proven to be effected by the surface roughness of the implant placed (Tetè *et al.*, 2008). Surface roughness greatly impacts the integrity of cells and the biomolecules present adjacent to the implant surface (Le Guéhenec *et al.*, 2007). Various studies reflect on the importance of treated or roughened surfaces in comparison to machined or polished ones (Le Guéhenec *et al.*, 2007; Wennerberger *et al.*, 2009). Sandblasting and acid etching were performed on the gritted surfaces to initially roughen the surfaces so that the samples could resemble commercial implant surfaces at the beginning of the study. The eventual morphology that was attained in our research was similar to a study done in 2005 by Anselme *et al.*, where it was proven that rougher surfaces prove to have lasting effects on osseointegration *in vitro* (Anselme *et al.*, 2005).

During the sandblasting process the impact of these particles with a titanium surface scrapes off the top layer of the substrate and creates craters of plastic deformation on the impacted spots. The degree of deformation depends upon the projected particle composition, size, nature and history of the target surface (Wennerberg *et al.*, 1996). The typical average roughness of blasted surfaces varies between 0.6 $\mu\text{m}$  and 3 $\mu\text{m}$  in dental endo-prostheses but can reach even 6 $\mu\text{m}$  when applied to orthopaedic prostheses. Sandblasting can result in anisotropic surface characteristics depending on the time of exposure and positioning of the sample with respect to the particle jet. After sandblasting, a number of the projected particles remain embedded on

the substrate surface and this alters its chemical properties (Anselme *et al.*, 2005; Marinho *et al.*, 2003). This substrate heterogeneity has been reported to reduce the corrosion resistance and even impair cell function and mineralization (Wang *et al.*, 2012). Therefore, nowadays the most used sandblasted protocols include an acid etching post-cleaning step that contributes to dissolve at least some of the projected particles (D. Cochran *et al.*, 1998; Roehling *et al.*, 2015).

In 2000, Orsini *et al.* conducted a study that compared the *in vitro* cell response of 10 machined and 10 sandblasted and acid-etched samples. It was concluded that morphologic irregularities induced by sandblasting and acid etching could improve initial cell anchorage, providing better osseointegration (Orsini *et al.*, 2000). Acid etching is based on the selective dissolution of the substrate grains after dissolution of the native oxide layer producing micron sized roughness (Novaes Jr *et al.*, 2010). Hence, in this study it was possible to achieve samples that were morphologically sound and free from alumina particles. The roughness achieved in this study coincides with commercially available implant surfaces and with studies that promote the presence of a roughened surface on an implant to enhance osseointegration (Anselme *et al.*, 2005; Orsini *et al.*, 2000; Rosa *et al.*, 2012).

## **5.2 Surface Characterization**

### **5.2.1 SBF – HA Coating**

A roughened surface coated with HA was employed as the control for this study because of HA's proven success in implant therapy (Kulkarni *et al.*, 2014; S.-W. Lee *et al.*, 2014). An SBF was used to coat the surfaces with HA. This method comes under biomimetic deposition of HA onto a surface. This biomimetic approach uses nature as its guide and helps in securing stable HA coatings that have proven osteoconductive properties (Sørensen *et al.*, 2015). In this

study, Tas-SBF in particular was used to form the HA layer on to the CPTi samples. This was done so because with the TRIS buffered Tas-SBF we were able to attain the HA crystallinity and morphology similar to that of bone-like apatite (Gandolfi *et al.*, 2015a; Jalota *et al.*, 2006; Nazir *et al.*, 2015). The *Sa* of the HA coated samples had increased in roughness after they were immersed in Tas-SBF for 14 days. This was beneficial consequently for the study because it promoted better results in the *in vitro* part of the experiment when cell attachment, proliferation and morphology were analysed. The FTIR spectrum indicated typical peaks for the presence of HA/Tricalcium phosphate on the surface of the samples. The EDS analysis further confirmed these findings. Hence, in this study a crystalline, bioactive and relatively uniform coating was achieved at the beginning of the surface characterization phase.

The crystallinity and the eventual roughness of a sample coated by the SBF technique is dependent on the duration of the immersion of the sample in the solution. Usually the surfaces to be experimented upon are immersed in the SBF solution for fourteen days to achieve a phase of HA that is stable and possesses greater similarity to natural bone apatite (Oscar *et al.*, 2015). Hence, in this study, the samples were immersed in the Tas-SBF solution for fourteen days. However, there are a few other studies that have reported reduced immersion times of titanium samples in SBF by changing the concentration and the ingredients of the solution in question. This has yielded considerably apt deposits of HA/Tricalcium Phosphate (Lee *et al.*, 2014; Tas & Bhaduri, 2004).

The present study adhered to the standard protocols of Tas-SBF and it was found that in fourteen days the crystallinity and the morphology of the HA/Tricalcium Phosphate was favourable while using the standard Tas-SBF solution. These favourable conditions for HA deposition were enhanced by creating samples that had unreactive surfaces causing no or

negligible effect on the final composition, morphology and crystallinity of the HA coating. This study proved that with samples that have been immersed in Tas-SBF for fourteen days, it is possible to achieve uniform HA/Tricalcium Phosphate coatings. This biomimetic coating was compositionally and structurally similar to the HA found in human bone. Our findings also coincided with a study conducted by Rigo *et al.* that tested the *in vitro* and *in vivo* success of biomimetic coatings (Rigo *et al.*, 2004).

### 5.2.2. Collagen Type I Coating

After obtaining a layer of HA/Tricalcium Phosphate layer on top of the CPTi samples, this study aimed at adding Type I Collagen on top of one of the groups that were being tested *in vitro*. There have been various researches that have demonstrated the osteogenic potential of biomimetically enhancing implant surfaces with Type I Collagen coatings (Becker *et al.*, 2009; Schliephake *et al.*, 2005; Stadlinger *et al.*, 2008). Type I Collagen contains a polypeptide backbone that is helical in nature. This helical architecture consists of approximately a thousand amino acids. Collagen is a crucial component of the human body and acts as a template for bio-mineralization. It also aids in mechanical stability and governs cell adhesion and migration. Additionally, it is necessary for general tissue support for hemostasis and repair (Goissis *et al.*, 1999). Therefore, these properties compel researchers to employ collagen as a coating material for osteoconductive and osteoinductive surfaces. The structural attributes of the coatings require specific techniques to spread the coating onto the surface and to stabilize this formation by cross-linkages.

In this study, HA and Type I Collagen were used in conjunction with each other as coating materials. There are various studies which suggest that the composite of these materials

increases osteoblast differentiation and enhances osteogenesis (Wahl *et al.*, 2006). An added advantage of using the composite of HA and Type I Collagen on titanium surfaces is that both of these materials are biocompatible (Scabbia *et al.*, 2004). Furthermore, HA and collagen together compensate for each other's physical and mechanical properties, that is, the ductility of collagen aids in providing greater fracture toughness to HA (Miguez *et al.*, 2004). This study was able to achieve a uniform layer of collagen on top of a Tas-SBF generated HA layer. These tried and tested benefits of the collagen layer on HA provided great results eventually. It was possible in this study to achieve a scaffolding of collagen morphologically.

### 5.2.3. RGD Coating

In this study, a group of samples was created that consisted of HA coated with RGD peptide. RGD was placed successfully on the HA surface through physical adsorption and provided a uniformly peptide covered surface that the cells could act upon. This peptide was used with the biomimetic strategy in mind that aims at the bio-activation of titanium surfaces by utilizing peptides that consist of the least amount of functional sequences of the progenitor protein (Hynes, 2002; Ryu *et al.*, 2013). This is consistent with a study conducted in 2009 by Straley *et al.* in which RGD was coated onto the surfaces with physical adsorption and this preparation of samples proved to be adjustable, quantifiable, and reproducible for *in vitro* studies (Straley *et al.*, 2009).

### **5.3 *In Vitro* Cell Response**

#### *5.3.1 Cell Viability*

Osseointegration of implants is usually researched *in vivo* on live animal samples and the data provided can be histomorphometrical or biomechanical. Due to the difficulty of this way of investigating osseointegration, osteoblastic cells are used *in vitro* to measure the effects of the initial stages of osseointegration. There are many studies that assess cellular osteoblastic interactions on titanium surfaces. Human osteoblasts were used in this study because these cells produce a greater degree of ALP activity when mineralization of the extracellular matrix occurs (Brammer *et al.*, 2011). Researchers suggest that the composition and the roughness of a surface affects initial cell viability, differentiation and spreading (Liet *al.*, 1996). Hence, in this experiment, the CPTi surfaces were altered and when the HOB cells were seeded onto the surfaces, the cell viability increased in all the groups except in the HA group, as seen by the MTT Assay results. The reason could be because of faulty equipment during the MTT Assay readings on various days of the study. This fact can be linked to the experimental contradiction that other studies have shown for titanium and HA, that is, there has been great cell response with solely HA as the surface coating (Le Guéhenec *et al.*, 2007).

The RGD and the Collagen group showed almost similar cell viability, except for an anomalous reading for the RGD sample. Again, faulty equipment during the procedure of the microplate readings for the MTT Assay may be the cause of these results because the beneficial effects of the composite materials were hypothesized to yield a greater degree of cell response.

Comparatively, the best results for the cell viability were for the Collagen group. For the samples that produced anomalous results, cell crowding and the phase of where the cells are in the cell cycle can be the main culprits (Cheng *et al.*, 2011).

### 5.3.2. Cell Differentiation

The ALP Assay was used to assess the cell differentiation (Jeong & Jeong, 2016). The results showed that the all samples showed similar values of absorbance in the first week but the second week showed an increased amount of absorbance for the Collagen group. This coincides with other studies (Chen *et al.*, 2016; Montesi *et al.*, 2016). The RGD group did not show greater values of absorbance and stayed nearer to the values of the HA group in the last week of the experiment too. The RGD group showed considerable cell viability but in the cell differentiation analyses, it did not compare as well as it was hypothesized in the beginning of the study. This coincides with Hennessy *et al.* who demonstrated that when RGD is presented in combination with adsorbed tibial proteins, it has a detrimental consequence on cell adhesion and proliferation. Moreover, analyses of HA disks implanted for 5 days showed that RGD significantly inhibits total bone formation as well as the amount of new bone directly contacting the implant perimeter. Thus, RGD, which is widely believed to promote cell/biomaterial interactions, has a negative effect on HA implant performance (Hennessy *et al.*, 2008).

There is a lot of literature that proves that certain peptide coated surfaces have an effect on short-term and long-term cell responses. In earlier implant healing studies, it was hypothesized that adding multiple active amino acid sequences to implants could introduce a selective competition between these active peptides and the binding domains of the native proteins. Contrarily, simplistic peptide sequences are not able to induce strong integrin signaling. Hence,

some studies have gone as far as to say that an implant surfaces that have cells bound to the peptides instead of proteins do not induce cell adhesion and may even compromise osseointegration (Tejero *et al.*, 2014).

### 5.3.3. Mineralization

In this study, the test done to prove and compare mineralization on the three groups of surfaces was Alizarin Red S. staining (Mariscal-Muñoz *et al.*, 2016). The greatest mineralization was found on the samples in the Collagen group. This is in coherence with other studies that aim to induce an osteogenic response *in vitro* (Venugopal, 2008). For example, when Prabhakaran *et al.* tried to compare nanofibers coated with HA and Collagen, the results showed that the composite of HA and collagen on a nano-fibrous scaffold could potentially induce cell proliferation and mineralization of osteoblasts, hence enhancing bone regeneration (Prabhakaran *et al.*, 2009). The RGD and HA groups had an almost a similar response of mineralization to each other.

### 5.3.4. Limitations Of The Study

If other methods of coating the surface with HA could be used, for example, plasma spraying or sol-gel method, it would have been interesting to discover which one works best *in vitro* when it is additionally coated with collagen.

### 5.3.5. Recommendations For Future Studies

We recommend that the CPTi surfaces be coated with a wider range peptides and proteins. It would be interesting to assess which coating can effectively change the course of implantology.

## CHAPTER 6 – CONCLUSION

In conclusion, collagen modified titanium surfaces yield a greater degree of osseointegration in comparison to RGD and HA coated surfaces. Collagen in conjunction with HA on CPTi surfaces can drastically enhance osseointegration *in vitro*. Collagen modified titanium surfaces yield a greater degree of osseointegration and produce more stable scaffolds on the implant surface when compared with RGD and HA/Tricalcium Phospahte coated CPTi surfaces *in vitro*. More research on this topic is advocated in the future so that the *in vivo* effects of these surface coating materials can be evaluated.

## REFERENCES

- Al-Haddad, A., Kutty, M. G., Abu Kasim, N. H., & Che Ab Aziz, Z. A. (2015). Physicochemical Properties of Calcium Phosphate Based Coating on Gutta-Percha Root Canal Filling. *International Journal of Polymer Science*, 2015, 5.
- Albrektsson, T., Brånemark, P.-I., Hansson, H.-A., & Lindström, J. (1981). Osseointegrated titanium implants: requirements for ensuring a long-lasting, direct bone-to-implant anchorage in man. *Acta Orthopaedica Scandinavica*, 52(2), 155-170.
- Albrektsson, T., & Johansson, C. (2001). Osteoinduction, osteoconduction and osseointegration. *European Spine Journal*, 10(2), S96-S101.
- Anderson, N. L., & Anderson, N. G. (2002). The human plasma proteome history, character, and diagnostic prospects. *Molecular & cellular proteomics*, 1(11), 845-867.
- Anitua, E., Troya, M., & Orive, G. (2012). Plasma rich in growth factors promote gingival tissue regeneration by stimulating fibroblast proliferation and migration and by blocking transforming growth factor-beta1-induced myodifferentiation. *J Periodontol*, 83(8), 1028-1037. doi: 10.1902/jop.2011.110505
- Anselme, K., & Bigerelle, M. (2005). Topography effects of pure titanium substrates on human osteoblast long-term adhesion. *Acta Biomaterialia*, 1(2), 211-222.
- Ao, H.-Y., Xie, Y.-T., Yang, S.-B., Wu, X.-D., Li, K., Zheng, X.-B., & Tang, T.-T. (2016). Covalently immobilised type I collagen facilitates osteoconduction and osseointegration of titanium coated implants. *Journal of Orthopaedic Translation*, 5, 16-25.
- Bailey, A., & Robins, S. (1975). Current topics in the biosynthesis, structure and function of collagen. *Science progress*, 63(251), 419-444.
- Banakh, O., Journot, T., Gay, P.-A., Matthey, J., Csefalvay, C., Kalinichenko, O., . . . Snizhko, L. (2016). Synthesis by anodic-spark deposition of Ca-and P-containing films on pure titanium and their biological response. *Applied Surface Science*, 378, 207-215.
- Barbas, A. (2016). Method for the surface treatment of titanium bone implants using, in order, a sodium hydroxide bath and anodization: Google Patents.
- Bateman, A. C., & Carr, N. (2008). *The Flesh and Bones of Pathology*: Elsevier Health Sciences.

- Becker, J., Al-Nawas, B., Klein, M. O., Schliephake, H., Terheyden, H., & Schwarz, F. (2009). Use of a new cross-linked collagen membrane for the treatment of dehiscence-type defects at titanium implants: a prospective, randomized-controlled double-blinded clinical multicenter study. *Clinical Oral Implants Research*, 20(7), 742-749.
- Bornstein, M. M., Valderrama, P., Jones, A. A., Wilson, T. G., Seibl, R., & Cochran, D. L. (2008). Bone apposition around two different sandblasted and acid-etched titanium implant surfaces: a histomorphometric study in canine mandibles. *Clinical Oral Implants Research*, 19(3), 233-241.
- Brammer, K. S., Choi, C., Frandsen, C. J., Oh, S., Johnston, G., & Jin, S. (2011). Comparative cell behavior on carbon-coated TiO<sub>2</sub> nanotube surfaces for osteoblasts vs. osteo-progenitor cells. *Acta Biomaterialia*, 7(6), 2697-2703.
- Branemark, P.-I. (1983). Osseointegration and its experimental background. *The Journal of prosthetic dentistry*, 50(3), 399-410.
- Brett, P., Harle, J., Salih, V., Mihoc, R., Olsen, I., Jones, F., & Tonetti, M. (2004). Roughness response genes in osteoblasts. *Bone*, 35(1), 124-133.
- Brunski, J. B. (1999). In vivo bone response to biomechanical loading at the bone/dental-implant interface. *Adv Dent Res*, 13, 99-119.
- Buser, D., Brogini, N., Wieland, M., Schenk, R., Denzer, A., Cochran, D., . . . Steinemann, S. (2004). Enhanced bone apposition to a chemically modified SLA titanium surface. *Journal of dental research*, 83(7), 529-533.
- Chen, L., Hu, J., Ran, J., Shen, X., & Tong, H. (2016). Synthesis and cytocompatibility of collagen/hydroxyapatite nanocomposite scaffold for bone tissue engineering. *Polymer Composites*, 37(1), 81-90.
- Cheng, Y. H., Chitteti, B. R., Streicher, D. A., Morgan, J. A., Rodriguez-Rodriguez, S., Carlesso, N., . . . Kacena, M. A. (2011). Impact of maturational status on the ability of osteoblasts to enhance the hematopoietic function of stem and progenitor cells. *Journal of Bone and Mineral Research*, 26(5), 1111-1121.
- Cho, Y.-D., Kim, S., Bae, H., Yoon, W., Kim, K., Ryoo, H., . . . Ku, Y. (2016). Biomimetic approach to stimulate osteogenesis on titanium implant surfaces using fibronectin derived oligopeptide. *Current pharmaceutical design*.

- Chrcanovic, B. R., Pedrosa, A. R., & Martins, M. D. (2012). Chemical and topographic analysis of treated surfaces of five different commercial dental titanium implants. *materials research*, 15(3), 372-382.
- Cochran, D., Schenk, R., Lussi, A., Higginbottom, F., & Buser, D. (1998). Bone response to unloaded and loaded titanium implants with a sandblasted and acid-etched surface: a histometric study in the canine mandible. *Journal of biomedical materials research*, 40(1), 1-11.
- Cochran, D. L., Buser, D., Ten Bruggenkate, C. M., Weingart, D., Taylor, T. M., Bernard, J. P., . . . Simpson, J. P. (2002). The use of reduced healing times on ITI® implants with a sandblasted and acid-etched (SLA) surface. *Clinical Oral Implants Research*, 13(2), 144-153.
- Davies, J. E. (2003). Understanding peri-implant endosseous healing. *J Dent Educ*, 67(8), 932-949.
- De Arriba, C., Tabuenca, J., Rodriguez-Torres, R., Fernandez-Valencia, R., Carrascosa-Sanchez, J., & Gomez-Pellico, L. (2016). Influence of osteoporosis on osseointegration: An experimental study. *European Journal of Anatomy*, 4(2), 61-67.
- Dimitriou, R., Tsiridis, E., & Giannoudis, P. V. (2005). Current concepts of molecular aspects of bone healing. *Injury*, 36(12), 1392-1404.
- Ducheyne, P., & Cuckler, J. M. (1992). Bioactive ceramic prosthetic coatings. *Clinical orthopaedics and related research*, 276, 102-114.
- Ferraz, M., Monteiro, F., & Manuel, C. (2004). Hydroxyapatite nanoparticles: a review of preparation methodologies. *Journal of Applied Biomaterials and Biomechanics*, 2(2), 74-80.
- Friedl, P., & Brocker, E. B. (2000). T cell migration in three-dimensional extracellular matrix: guidance by polarity and sensations. *Dev Immunol*, 7(2-4), 249-266.
- Gandolfi, M., Taddei, P., Siboni, F., Perrotti, V., Iezzi, G., Piattelli, A., & Prati, C. (2015a). Micro-topography and reactivity of implant surfaces: an in vitro study in simulated body fluid (SBF). *Microscopy and Microanalysis*, 21(01), 190-203.
- Gandolfi, M., Taddei, P., Siboni, F., Perrotti, V., Iezzi, G., Piattelli, A., & Prati, C. (2015b). Micro-Topography and Reactivity of Implant Surfaces: An In Vitro Study in Simulated Body Fluid (SBF). *Microscopy and Microanalysis*, 1-14.

- Geissler, U., Hempel, U., Wolf, C., Scharnweber, D., Worch, H., & Wenzel, K. W. (2000). Collagen type I-coating of Ti6Al4V promotes adhesion of osteoblasts. *Journal of biomedical materials research*, 51(4), 752-760.
- Goissis, G., Marcantonio, E., Marcantônio, R. A. C., Lia, R. C. C., Cancian, D. C., & de Carvalho, W. M. (1999). Biocompatibility studies of anionic collagen membranes with different degree of glutaraldehyde cross-linking. *Biomaterials*, 20(1), 27-34.
- Hennessy, K. M., Clem, W. C., Phipps, M. C., Sawyer, A. A., Shaikh, F. M., & Bellis, S. L. (2008). The effect of RGD peptides on osseointegration of hydroxyapatite biomaterials. *Biomaterials*, 29(21), 3075-3083.
- Hersel, U., Dahmen, C., & Kessler, H. (2003). RGD modified polymers: biomaterials for stimulated cell adhesion and beyond. *Biomaterials*, 24(24), 4385-4415.
- Hotchkiss, K. M., Ayad, N. B., Hyzy, S. L., Boyan, B. D., & Olivares-Navarrete, R. (2016). Dental implant surface chemistry and energy alter macrophage activation in vitro. *Clinical Oral Implants Research*.
- Hynes, R. O. (1992). Integrins: versatility, modulation, and signaling in cell adhesion. *Cell*, 69(1), 11-25.
- Hynes, R. O. (2002). Integrins: bidirectional, allosteric signaling machines. *Cell*, 110(6), 673-687.
- Jalota, S., Bhaduri, S., & Tas, A. (2006). Effect of carbonate content and buffer type on calcium phosphate formation in SBF solutions. *Journal of Materials Science: Materials in Medicine*, 17(8), 697-707.
- Jeong, S.-J., & Jeong, M.-J. (2016). Effect of Thymosin  $\beta$ 4 on the Differentiation and Mineralization of MC3T3-E1 Cell on a Titanium Surface. *Journal of Nanoscience and Nanotechnology*, 16(2), 1979-1983.
- Jonášová, L., Müller, F. A., Helebrant, A., Strnad, J., & Greil, P. (2004). Biomimetic apatite formation on chemically treated titanium. *Biomaterials*, 25(7), 1187-1194.
- Junker, R., Dimakis, A., Thoneick, M., & Jansen, J. A. (2009). Effects of implant surface coatings and composition on bone integration: a systematic review. *Clinical Oral Implants Research*, 20(s4), 185-206.

- Kämmerer, T. A., Palarie, V., Schiegnitz, E., Topalo, V., Schröter, A., Al-Nawas, B., & Kämmerer, P. W. (2016). A biphasic calcium phosphate coating for potential drug delivery affects early osseointegration of titanium implants. *Journal of Oral Pathology & Medicine*.
- Karamian, E., Khandan, A., Researchers, Y., Club, E., Branch, K., & Motamedi, M. R. K. (2002). Surface Characteristics and Bioactivity of A Novel Natural HA/Zircon Nanocomposite. *materials research*, 59(2), 312-317.
- Knabe, C., Klar, F., Fitzner, R., Radlanski, R., & Gross, U. (2002). In vitro investigation of titanium and hydroxyapatite dental implant surfaces using a rat bone marrow stromal cell culture system. *Biomaterials*, 23(15), 3235-3245.
- Kokubo, T., Kushitani, H., Sakka, S., Kitsugi, T., & Yamamuro, T. (1990). Solutions able to reproduce in vivo surface-structure changes in bioactive glass-ceramic A-W3. *Journal of biomedical materials research*, 24(6), 721-734.
- Kokubo, T., & Takadama, H. (2008). Simulated body fluid (SBF) as a standard tool to test the bioactivity of implants. *Handbook of Biomineralization: Biological Aspects and Structure Formation*, 97-109.
- Kulkarni, M., Mazare, A., Schmuki, P., Iglíč, A., & Seifalian, A. (2014). Biomaterial surface modification of titanium and titanium alloys for medical applications. *Nanomedicine*, 111, 111.
- Kulkarni, M., Mazare, A., Schmuki, P., Iglíč, A., & Seifalian, A. (2014). Biomaterial surface modification of titanium and titanium alloys for medical applications. *Nanomedicine*, 111, 111.
- Lavenus, S., Louarn, G., & Layrolle, P. (2010). Nanotechnology and dental implants. *International journal of biomaterials*, 2010.
- Le Guéhennec, L., Soueidan, A., Layrolle, P., & Amouriq, Y. (2007). Surface treatments of titanium dental implants for rapid osseointegration. *Dental materials*, 23(7), 844-854.
- Lee, B.-A., Kim, H.-J., Xuan, Y.-Z., Park, Y.-J., Chung, H.-J., & Kim, Y.-J. (2014). Osteoblastic behavior to zirconium coating on Ti-6Al-4V alloy. *The journal of advanced prosthodontics*, 6(6), 512-520.
- Lee, J. H., Madden, A. S., Kriven, W. M., & Tas, A. C. (2014). Synthetic Aragonite (CaCO<sub>3</sub>) as a Potential Additive in Calcium Phosphate Cements: Evaluation in Tris-Free SBF at 37° C. *Journal of the American Ceramic Society*, 97(10), 3052-3061.

- Lee, S.-W., Hahn, B.-D., Kang, T. Y., Lee, M.-J., Choi, J.-Y., Kim, M.-K., & Kim, S.-G. (2014). Hydroxyapatite and Collagen Combination-Coated Dental Implants Display Better Bone Formation in the Peri-Implant Area Than the Same Combination Plus Bone Morphogenetic Protein-2-Coated Implants, Hydroxyapatite Only Coated Implants, and Uncoated Implants. *Journal of Oral and Maxillofacial Surgery*, 72(1), 53-60.
- Li, P., De Groot, K., & Kokubo, T. (1996). Bioactive Ca<sub>10</sub>(PO<sub>4</sub>)<sub>6</sub>(OH)<sub>2</sub>-TiO<sub>2</sub> composite coating prepared by sol-gel process. *Journal of Sol-Gel Science and Technology*, 7(1-2), 27-34.
- Liao, S., Li, B., Ma, Z., Wei, H., Chan, C., & Ramakrishna, S. (2006). Biomimetic electrospun nanofibers for tissue regeneration. *Biomedical Materials*, 1(3), R45.
- Lincks, J., Boyan, B., Blanchard, C., Lohmann, C., Liu, Y., Cochran, D., . . . Schwartz, Z. (1998). Response of MG63 osteoblast-like cells to titanium and titanium alloy is dependent on surface roughness and composition. *Biomaterials*, 19(23), 2219-2232.
- Marinho, V. C., Celletti, R., Bracchetti, G., Petrone, G., Minkin, C., & Piattelli, A. (2003). Sandblasted and acid-etched dental implants: a histologic study in rats. *International Journal of Oral & Maxillofacial Implants*, 18(1).
- Mariscal-Muñoz, E., Costa, C. A., Tavares, H. S., Bianchi, J., Hebling, J., Machado, J. P., . . . Souza, P. P. (2016). Osteoblast differentiation is enhanced by a nano-to-micro hybrid titanium surface created by Yb: YAG laser irradiation. *Clinical oral investigations*, 20(3), 503-511.
- Medvedev, A., Ng, H.-P., Lapovok, R., Estrin, Y., Lowe, T., & Anumalasetty, V. (2016). Effect of bulk microstructure of commercially pure titanium on surface characteristics and fatigue properties after surface modification by sand blasting and acid-etching. *Journal of the mechanical behavior of biomedical materials*, 57, 55-68.
- Miguez, P., Pereira, P., Atsawasuan, P., & Yamauchi, M. (2004). Collagen cross-linking and ultimate tensile strength in dentin. *Journal of dental research*, 83(10), 807-810.
- Montesi, M., & Panseri, S. (2016). Triggering Cell–Biomaterial Interaction: Recent Approaches for Osteochondral Regeneration. *Bio-Inspired Regenerative Medicine: Materials, Processes, and Clinical Applications*, 283.
- Monti, S. (2007). Molecular Dynamics Simulations of Collagen-like Peptide Adsorption on Titanium-Based Material Surfaces. *The Journal of Physical Chemistry C*, 111(16), 6086-6094.

- Nagai, M., Hayakawa, T., Fukatsu, A., Yamamoto, M., Fukumoto, M., Nagahama, F., . . . KATO, T. (2002). In vitro study of collagen coating of titanium implants for initial cell attachment. *Dental materials journal*, 21(3), 250-260.
- Nazir, M., Pei Ting, O., See Yee, T., Pushparajan, S., Swaminathan, D., & Kutty, M. G. (2015). Biomimetic Coating of Modified Titanium Surfaces with Hydroxyapatite Using Simulated Body Fluid. *Advances in Materials Science and Engineering*, 2015.
- Novaes Jr, A. B., Souza, S. L. S. d., Barros, R. R. M. d., Pereira, K. K. Y., Iezzi, G., & Piattelli, A. (2010). Influence of implant surfaces on osseointegration. *Brazilian dental journal*, 21(6), 471-481.
- Orsini, G., Assenza, B., Scarano, A., Piattelli, M., & Piattelli, A. (2000). Surface analysis of machined versus sandblasted and acid-etched titanium implants. *International Journal of Oral & Maxillofacial Implants*, 15(6).
- Oscar, D., Victor, B., J sica, Z., & Romina, G. (2015). *Comparative In Vitro Study of Surface Treatment of Grade II Titanium Biomedical Implant*. Paper presented at the VI Latin American Congress on Biomedical Engineering CLAIB 2014, Paran , Argentina 29, 30 & 31 October 2014.
- Park, J. Y., & Davies, J. E. (2000). Red blood cell and platelet interactions with titanium implant surfaces. *Clinical Oral Implants Research*, 11(6), 530-539.
- Pfaff, M. (1997). Recognition sites of RGD-dependent integrins *Integrin-ligand interaction* (pp. 101-121): Springer.
- Piattelli, A., Scarano, A., Corigliano, M., & Piattelli, M. (1996). Presence of multinucleated giant cells around machined, sandblasted and plasma-sprayed titanium implants: a histological and histochemical time-course study in rabbit. *Biomaterials*, 17(21), 2053-2058.
- Pierschbacher, M. D., & Ruoslahti, E. (1984). Cell attachment activity of fibronectin can be duplicated by small synthetic fragments of the molecule. *Nature*, 309(5963), 30.
- Prabhakaran, M. P., Venugopal, J., & Ramakrishna, S. (2009). Electrospun nanostructured scaffolds for bone tissue engineering. *Acta Biomaterialia*, 5(8), 2884-2893.
- Preshaw, P. (2015). Summary of: Implant surface characteristics and their effect on osseointegration. *British Dental Journal*, 218(5), 292-293.
- Ramachandran, G., & Kartha, G. (1954). Structure of collagen.

- Rammelt, S., Illert, T., Bierbaum, S., Scharnweber, D., Zwipp, H., & Schneiders, W. (2006). Coating of titanium implants with collagen, RGD peptide and chondroitin sulfate. *Biomaterials*, 27(32), 5561-5571.
- Raphel, J., Karlsson, J., Galli, S., Wennerberg, A., Lindsay, C., Haugh, M. G., . . . Andersson, M. (2016). Engineered protein coatings to improve the osseointegration of dental and orthopaedic implants. *Biomaterials*, 83, 269-282.
- Rigo, E. C. S., Boschi, A. O., Yoshimoto, M., Allegrini Jr, S., Konig Jr, B., & Carbonari, M. J. (2004). Evaluation in vitro and in vivo of biomimetic hydroxyapatite coated on titanium dental implants. *Materials Science and Engineering: C*, 24(5), 647-651.
- Roehling, S. K., Meng, B., & Cochran, D. L. (2015). Sandblasted and Acid-Etched Implant Surfaces With or Without High Surface Free Energy: Experimental and Clinical Background *Implant Surfaces and their Biological and Clinical Impact* (pp. 93-136): Springer.
- Rosa, M. B., Albrektsson, T., Francischone, C. E., Schwartz Filho, H. O., & Wennerberg, A. (2012). The influence of surface treatment on the implant roughness pattern. *Journal of Applied Oral Science*, 20(5), 550-555.
- Ryu, J.-J., Park, K., Kim, H.-S., Jeong, C.-M., & Huh, J.-B. (2013). Effects of anodized titanium with Arg-Gly-Asp (RGD) peptide immobilized via chemical grafting or physical adsorption on bone cell adhesion and differentiation. *International Journal of Oral & Maxillofacial Implants*, 28(4).
- Sammons, R. L., Lumbikanonda, N., Gross, M., & Cantzler, P. (2005). Comparison of osteoblast spreading on microstructured dental implant surfaces and cell behaviour in an explant model of osseointegration. *Clinical Oral Implants Research*, 16(6), 657-666.
- Sartori, M., Giavaresi, G., Parrilli, A., Ferrari, A., Aldini, N. N., Morra, M., . . . Fini, M. (2015). Collagen type I coating stimulates bone regeneration and osseointegration of titanium implants in the osteopenic rat. *International orthopaedics*, 39(10), 2041-2052.
- Sawyer, A. A., Hennessy, K. M., & Bellis, S. L. (2005). Regulation of mesenchymal stem cell attachment and spreading on hydroxyapatite by RGD peptides and adsorbed serum proteins. *Biomaterials*, 26(13), 1467-1475.

- Scabbia, A., & Trombelli, L. (2004). A comparative study on the use of a HA/collagen/chondroitin sulphate biomaterial (Biostite®) and a bovine-derived HA xenograft (Bio-Oss®) in the treatment of deep intra-osseous defects. *Journal of clinical periodontology*, 31(5), 348-355.
- Schliephake, H., Scharnweber, D., Dard, M., Sewing, A., Aref, A., & Roessler, S. (2005). Functionalization of dental implant surfaces using adhesion molecules. *Journal of Biomedical Materials Research Part B: Applied Biomaterials*, 73(1), 88-96.
- Shalabi, M., Gortemaker, A., Van't Hof, M., Jansen, J., & Creugers, N. (2006). Implant surface roughness and bone healing: a systematic review. *Journal of dental research*, 85(6), 496-500.
- Sörensen, J. H., Dürselen, L., Welch, K., Sörensen, T. C., Procter, P., Engqvist, H., . . . Steckel, H. (2015). Biomimetic hydroxyapatite coated titanium screws demonstrate rapid implant stabilization and safe removal in-vivo. *Journal of Biomaterials and Nanobiotechnology*, 6(01), 20.
- Stadlinger, B., Pilling, E., Huhle, M., Mai, R., Bierbaum, S., Scharnweber, D., . . . Eckelt, U. (2008). Evaluation of osseointegration of dental implants coated with collagen, chondroitin sulphate and BMP-4: an animal study. *International journal of oral and maxillofacial surgery*, 37(1), 54-59.
- Stanford, C. M. (2010). Surface modification of biomedical and dental implants and the processes of inflammation, wound healing and bone formation. *International journal of molecular sciences*, 11(1), 354-369.
- Straley, K. S., & Heilshorn, S. C. (2009). Design and adsorption of modular engineered proteins to prepare customized, neuron-compatible coatings. *Frontiers in Neuroengineering*, 2. doi: 10.3389/neuro.16.009.2009
- Suchanek, W., & Yoshimura, M. (1998). Processing and properties of hydroxyapatite-based biomaterials for use as hard tissue replacement implants. *Journal of Materials Research*, 13(01), 94-117.
- Tao, Z.-S., Zhou, W.-S., He, X.-W., Liu, W., Bai, B.-L., Zhou, Q., . . . Sun, T. (2016). A comparative study of zinc, magnesium, strontium-incorporated hydroxyapatite-coated titanium implants for osseointegration of osteopenic rats. *Materials Science and Engineering: C*, 62, 226-232.
- Tas, A. C., & Bhaduri, S. B. (2004). Rapid coating of Ti6Al4V at room temperature with a calcium phosphate solution similar to 10× simulated body fluid. *Journal of Materials Research*, 19(09), 2742-2749.

- Tejero, R., Anitua, E., & Orive, G. (2014). Toward the biomimetic implant surface: Biopolymers on titanium-based implants for bone regeneration. *Progress in Polymer Science*, 39(7), 1406-1447.
- Teng, F.-Y., Chen, W.-C., Wang, Y.-L., Hung, C.-C., & Tseng, C.-C. (2016). Effects of Osseointegration by Bone Morphogenetic Protein-2 on Titanium Implants In Vitro and In Vivo. *Bioinorganic chemistry and applications*, 2016.
- Terheyden, H., Lang, N. P., Bierbaum, S., & Stadlinger, B. (2012). Osseointegration – communication of cells. *Clinical Oral Implants Research*, 23(10), 1127-1135.
- Tetè, S., Mastrangelo, F., Traini, T., Vinci, R., Sammartino, G., Marenzi, G., & Gherlone, E. (2008). A Macro- and Nanostructure Evaluation of a Novel Dental Implant. *Implant Dentistry*, 17(3), 309-320.
- Venugopal, J. e. a. (2008). Mineralization of osteoblasts with electrospun collagen/hydroxyapatite nanofibers. *Journal of Materials Science: Materials in Medicine*, 19(5), 2039-2046.
- Villar, C. C., Huynh-Ba, G., Mills, M. P., & Cochran, D. L. (2011). Wound healing around dental implants. *Endodontic Topics*, 25(1), 44-62.
- Wahl, D., & Czernuszka, J. (2006). Collagen-hydroxyapatite composites for hard tissue repair. *Eur Cell Mater*, 11, 43-56.
- Wang, K., Zhou, C., Hong, Y., & Zhang, X. (2012). A review of protein adsorption on bioceramics. *Interface focus*, 2(3), 259-277.
- Webster, T. J., Ergun, C., Doremus, R. H., Siegel, R. W., & Bizios, R. (2000). Enhanced functions of osteoblasts on nanophase ceramics. *Biomaterials*, 21(17), 1803-1810.
- Webster, T. J., Siegel, R. W., & Bizios, R. (2000). Enhanced surface and mechanical properties of nanophase ceramics to achieve orthopaedic/dental implant efficacy. *Key Engineering Materials*, 192, 321-324.
- Wennerberg, A., & Albrektsson, T. (2009). Effects of titanium surface topography on bone integration: a systematic review. *Clinical Oral Implants Research*, 20(s4), 172-184.
- Wennerberg, A., Albrektsson, T., & Lausmaa, J. (1996). Torque and histomorphometric evaluation of cp titanium screws blasted with 25- and 75- $\mu$ m-sized particles of Al<sub>2</sub>O<sub>3</sub>. *Journal of biomedical materials research*, 30(2), 251-260.

- Whitehead, R. Y., Lacefield, W., & Lucas, L. (1993). Structure and integrity of a plasma sprayed hydroxylapatite coating on titanium. *Journal of biomedical materials research*, 27(12), 1501-1507.
- Xie, J., Baumann, M. J., & McCabe, L. R. (2004). Osteoblasts respond to hydroxyapatite surfaces with immediate changes in gene expression. *Journal of Biomedical Materials Research Part A*, 71(1), 108-117.
- Yang, C., Cheng, K., Weng, W., & Yang, C. (2009). Immobilization of RGD peptide on HA coating through a chemical bonding approach. *Journal of Materials Science: Materials in Medicine*, 20(11), 2349-2352.
- Yang, D. H., Lee, D. W., Kwon, Y. D., Kim, H. J., Chun, H. J., Jang, J. W., & Khang, G. (2015). Surface modification of titanium with hydroxyapatite–heparin–BMP-2 enhances the efficacy of bone formation and osseointegration in vitro and in vivo. *Journal of tissue engineering and regenerative medicine*, 9(9), 1067-1077.
- Yang, Y., Tian, J., Deng, L., & Ong, J. L. (2002). Morphological behavior of osteoblast-like cells on surface-modified titanium in vitro. *Biomaterials*, 23(5), 1383-1389.
- Zakaria, S. M., Sharif Zein, S. H., Othman, M. R., Yang, F., & Jansen, J. A. (2013). Nanophase hydroxyapatite as a biomaterial in advanced hard tissue engineering: a review. *Tissue Eng Part B Rev*, 19(5), 431-441. doi: 10.1089/ten.TEB.2012.0624
- Zhao, G., Zinger, O., Schwartz, Z., Wieland, M., Landolt, D., & Boyan, B. D. (2006). Osteoblast-like cells are sensitive to submicron-scale surface structure. *Clinical Oral Implants Research*, 17(3), 258-264.

## SUPPLEMENTARY

### *Publication and Conferences*

- **Biomimetic Coating of Modified Titanium Surfaces with Hydroxyapatite Using Simulated Body Fluid**, Advances in Materials Science and Engineering, Volume 2015 (2015), Article ID 407379.
- **1<sup>st</sup> Place** in ORAL PRESENTATION at IADR MALSEC Conference.
- ORAL PRESENTATION at the 1st International Conference in Innovative Dentistry (ICID 2015).

University of Malaya